

Supporting Information

For

# **Bis(4-carboxypyrazol-1-yl)acetic acid: A scorpionate ligand for complexes with improved water solubility**

Wintana Tzegai,<sup>[a]</sup> Michaela Reil,<sup>[a]</sup> and Nicolai Burzlaff\*<sup>[a]</sup>

<sup>[a]</sup>Inorganic Chemistry, Department of Chemistry and Pharmacy, Friedrich-Alexander-Universität Erlangen-Nürnberg (FAU), Egerlandstraße 1, 91058 Erlangen, Germany

## **Table of Contents**

- 1. Single Crystal X-ray Diffraction Experiments**
- 2. <sup>1</sup>H NMR and <sup>13</sup>C NMR spectra**
- 3. UV-vis spectra**
- 4. IR spectra**
- 5. MS data**
- 6. Elemental analyses**

## 1. Single Crystal X-ray Diffraction Experiments

**Table S1.** Methods and solvents used in the preparation of single crystals of ligand **2** and complexes **4 - 6**.

Compound	Technique	Solution in	Solvent for solvent diffusion	Temperature
<b>2</b>	liquid-liquid diffusion	tetrahydrofurane	<i>n</i> -pentane	ambient
<b>4</b>	liquid-liquid diffusion	acetonitrile	chloroform	ambient
<b>5</b>	liquid-liquid diffusion	acetone	dichloromethane	ambient
<b>6a-1</b>	liquid-liquid diffusion	methanol	diethylether	ambient
<b>6a-2</b>	slow evaporation	water	-	4°C

**Table S2.** Crystal data and refinement details of compounds **2** and **4-6**.

	<b>2</b>	<b>4</b>	<b>5</b>	<b>6a-1</b>	<b>6a-2</b>
CCDC number	2130703	2130704	2130706	2130707	2130708
empirical formula	C <sub>10</sub> H <sub>8</sub> N <sub>4</sub> O <sub>6</sub> × C <sub>4</sub> H <sub>8</sub> O	C <sub>13</sub> H <sub>7</sub> MnN <sub>4</sub> O <sub>9</sub>	C <sub>13</sub> H <sub>7</sub> N <sub>4</sub> O <sub>9</sub> Re × 0.5 H <sub>2</sub> O	C <sub>12</sub> H <sub>7</sub> ClN <sub>4</sub> O <sub>8</sub> Ru × CH <sub>4</sub> O	C <sub>12</sub> H <sub>7</sub> ClN <sub>4</sub> O <sub>8</sub> Ru × H <sub>2</sub> O
formula mass [g mol <sup>-1</sup> ]	352.31	418.17	558.43	503.78	489.75
crystal color/habit	colourless/ block	light yellow/ block	colourless/ block	metallic yellow/ block	yellow/ plate
crystal system	monoclinic	monoclinic	triclinic	monoclinic	monoclinic
space group, Z	<i>I</i> 2/ <i>a</i> , 8	<i>P</i> 2 <sub>1</sub> / <i>n</i> , 4	<i>P</i> -1, 8	<i>C</i> 2/ <i>c</i> , 8	<i>P</i> 2 <sub>1</sub> / <i>c</i> , 4
<i>a</i> [Å]	15.8518(3)	14.9306(5)	14.3811(5)	33.2013(8)	12.5010(2)
<i>b</i> [Å]	15.4697(4)	5.6066(2)	15.1010(5)	11.7943(3)	14.0811(2)
<i>c</i> [Å]	13.9712(2)	20.6630(8)	17.2257(6)	10.7307(2)	9.18410(10)
$\alpha$ [°]	90	90	107.251(3)	90	90
$\beta$ [°]	100.252(2)	107.404(4)	94.748(3)	96.218(2)	93.0360(10)
$\gamma$ [°]	90	90	110.515(3)	90	90
<i>V</i> [Å <sup>3</sup> ]	3371.35(12)	1650.51(11)	3272.3(2)	4177.27(17)	1614.39(4)
$\theta$ [°]	4.025 to 72.726	3.238 to 72.278	2.747 to 72.529	3.980 to 72.544	3.541 to 72.586
<i>h</i>	-19 to 19	-18 to 18	-17 to 17	-40 to 37	-15 to 8
<i>k</i>	-19 to 18	-6 to 6	-13 to 18	-14 to 10	-17 to 16
<i>l</i>	-17 to 11	-17 to 25	-21 to 16	-13 to 10	-11 to 11
<i>F</i> (000)	1472	840	2120	2000	968
$\mu$ (Cu-K $\alpha$ ) [mm <sup>-1</sup> ]	0.970	7.077	15.146	7.726	9.973
crystal size [mm]	0.451 × 0.131 × 0.099	0.107 × 0.078 × 0.031	0.075 × 0.062 × 0.026	0.366 × 0.083 × 0.081	0.248 × 0.115 × 0.076
<i>D</i> <sub>c</sub> [g cm <sup>-3</sup> ], <i>T</i> [K]	1.388, 99.99(10)	1.683, 99.9(3)	2.267, 99.9(4)	1.602, 99.9(5)	2.015, 99.9(4)
reflections collected	9810	7946	21454	8112	5952
independent reflections	3302	3171	12476	4030	3100
obs. Reflections, <i>I</i> > 2 $\sigma$ <i>I</i>	2949	2540	10901	3810	2970
Parameters, restraints	348, 296	246, 0	1008, 0	262, 19	260, 21
weight parameter <i>a</i>	0.0652	0.0382	0.0291	0.0611	0.0458
weight parameter <i>b</i>	4.7913	0.4141	1.6826	19.7346	1.4266
<i>R</i> <sub>1</sub> (observed)	0.0508	0.0415	0.0305	0.0423	0.0290
<i>R</i> <sub>1</sub> (overall)	0.0552	0.0589	0.0381	0.0438	0.0300
<i>wR</i> <sub>2</sub> (observed)	0.1306	0.0907	0.0698	0.1113	0.0759
<i>wR</i> <sub>2</sub> (overall)	0.1345	0.0991	0.0733	0.1128	0.0768
diff. peak/hole [e/Å]	0.713/ -0.379	0.392/ -0.346	1.894/ -1.299	1.207/ -0.778	0.970/ -1.058
goodness-of-fit on <i>F</i> <sup>2</sup>	1.061	1.040	1.036	1.041	1.058

**Table S3.** Selected bond lengths and angles of molecular structure of H<sub>3</sub>bcpza (**2**).

Selected bond lengths [Å]	H <sub>3</sub> bcpza ( <b>2</b> )
C2–O1	1.275(3)
C2–O2	1.232(3)
N11–N12	1.362(2)
N11–C12	1.324(2)
C12–C13	1.406(2)
O11–C16	1.322(2)
O12–C16	1.216(2)
Selected angles [°]	
N12–C1–C2	111.63(14)
N11–N12–C1	118.85(13)

**Table S4.** Selected bond lengths and angles of molecular structure of [Mn(H<sub>2</sub>bcpza)(CO)<sub>3</sub>] (**4**).

Selected bond lengths [Å]	[Mn(H <sub>2</sub> bcpza)(CO) <sub>3</sub> ] ( <b>4</b> )
Mn–O1	2.061(2)
Mn–N11	2.041(3)
Mn–N21	2.051(2)
Mn–C3	1.818(3)
Mn–C4	1.809(3)
Mn–C5	1.809(3)
Selected angles [°]	
O1–Mn–N11	85.61(9)
O1–Mn–N21	84.72(9)
N11–Mn–N21	84.54(10)

**Table S5.** Selected bond lengths and angles of molecular structure of  $[\text{Re}(\text{H}_2\text{bcpza})(\text{CO})_3]$  (**5**). The four independent molecules in the asymmetric unit are marked with superscripts **a-d**.

Selected bond lengths [Å]	$[\text{Re}(\text{H}_2\text{bcpza})(\text{CO})_3]$ ( <b>5</b> )
Re–O1	2.189(3) <sup>a</sup> , 2.154(3) <sup>b</sup> , 2.168(3) <sup>c</sup> , 2.172(4) <sup>d</sup>
Re–N11	2.181(4) <sup>a</sup> , 2.187(4) <sup>b</sup> , 2.182(4) <sup>c</sup> , 2.194(5) <sup>d</sup>
Re–N21	2.183(5) <sup>a</sup> , 2.163(4) <sup>b</sup> , 2.186(4) <sup>c</sup> , 2.158(4) <sup>d</sup>
Re–C3	1.937(6) <sup>a</sup> , 1.927(6) <sup>b</sup> , 1.924(6) <sup>c</sup> , 1.937(6) <sup>d</sup>
Re–C4	1.903(6) <sup>a</sup> , 1.909(6) <sup>b</sup> , 1.902(6) <sup>c</sup> , 1.905(6) <sup>d</sup>
Re–C5	1.915(6) <sup>a</sup> , 1.916(6) <sup>b</sup> , 1.929(5) <sup>c</sup> , 1.945(6) <sup>d</sup>
Selected angles [°]	
O1–Re–N11	81.80(14) <sup>a</sup> , 82.83(14) <sup>b</sup> , 80.80(14) <sup>c</sup> , 78.80(15) <sup>d</sup>
O1–Re–N21	80.17(15) <sup>a</sup> , 80.30(15) <sup>b</sup> , 80.82(14) <sup>c</sup> , 83.44(15) <sup>d</sup>
N11–Re–N21	80.61(16) <sup>a</sup> , 82.68(15) <sup>b</sup> , 82.04(15) <sup>c</sup> , 82.08(16) <sup>d</sup>

**Table S6.** Selected distances and angles of molecular structure of  $[\text{Ru}(\text{H}_2\text{bcpza})\text{Cl}(\text{CO})_2]$  (**6a-1** + **6a-2**).

Selected bond lengths [Å]	$[\text{Ru}(\text{H}_2\text{bcpza})\text{Cl}(\text{CO})_2]$ ( <b>6a-1</b> )	$[\text{Ru}(\text{H}_2\text{bcpza})\text{Cl}(\text{CO})_2]$ ( <b>6a-2</b> )
Ru–O1	2.108(3)	2.1123(19)
Ru–N11	2.118(3)	2.118(2)
Ru–N21	2.099(3)	2.131(2)
Ru–C3	1.956(5)	1.934(3)
Ru–C4	1.919(4)	1.910(3)
Ru–Cl	2.3690(11)	2.3596(8)
Selected angles [°]		
O1–Ru–N11	85.28(11)	85.24(8)
N21–Ru–O1	85.50(11)	85.47(7)
N21–Ru–N11	83.78(12)	83.76(9)

## 2. $^1\text{H}$ NMR and $^{13}\text{C}$ NMR spectra

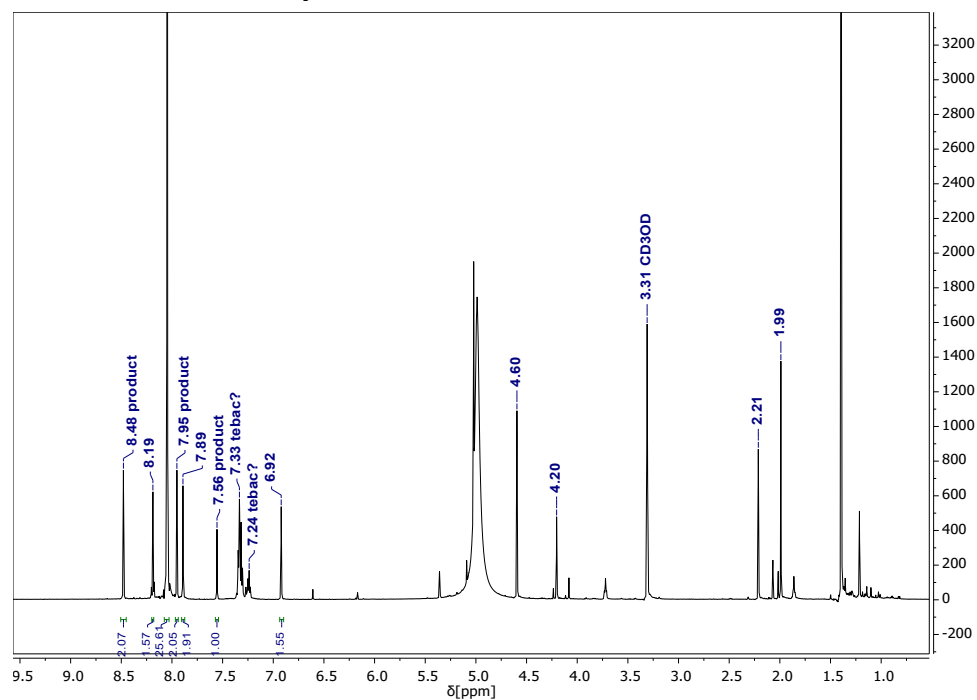


**Figure S1.**  $^1\text{H}$  NMR spectrum (methanol- $\text{d}_4$ ) of the extracted organic phase regarding the attempted synthesis of  $\text{H}_3\text{bcpza}$  (**2**) by using pyrazole-4-carboxylic acid as precursor.

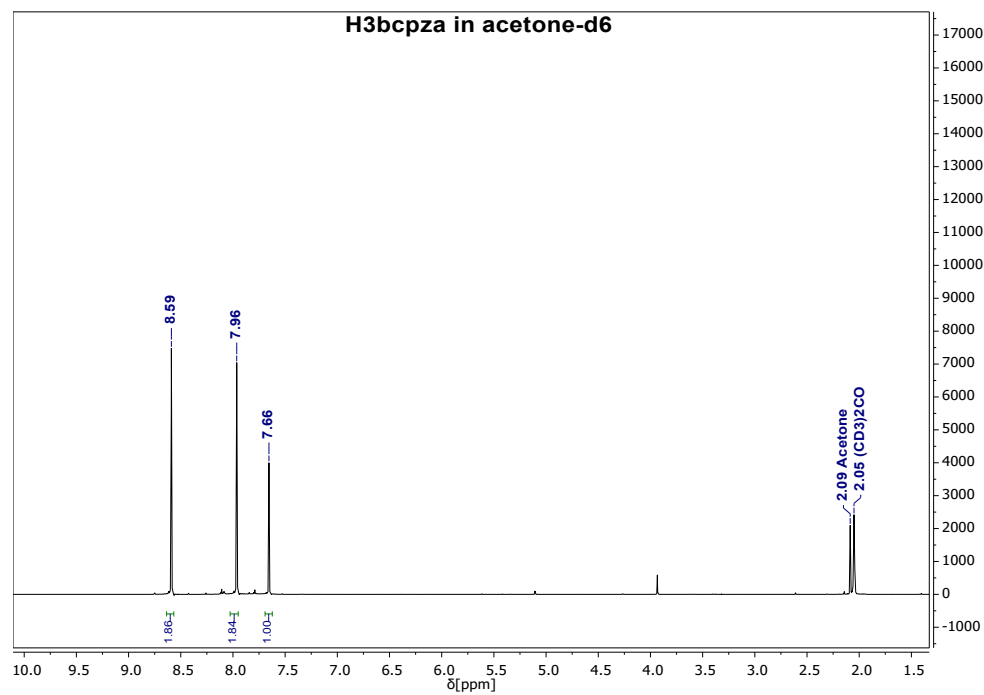


**Figure S2.**  $^1\text{H}$  NMR spectrum of  $\text{H}_3\text{bcpza}$  (**2**) in acetone- $\text{d}_6$ .

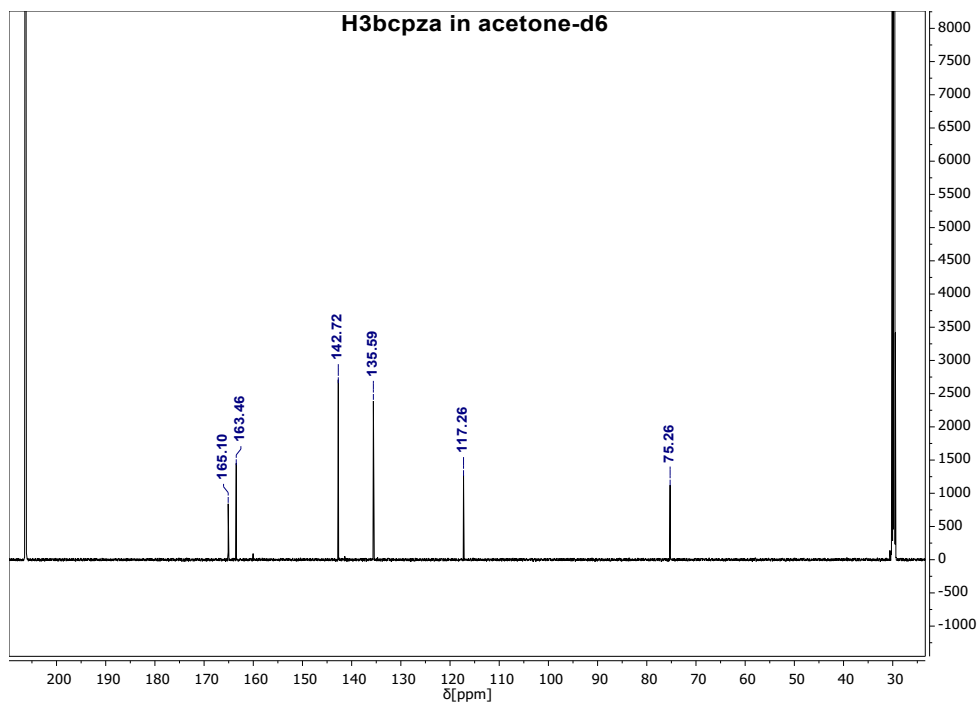


Figure S3.  $^{13}\text{C}$  NMR spectrum of H<sub>3</sub>bcpza (**2**) in acetone-d<sub>6</sub>.

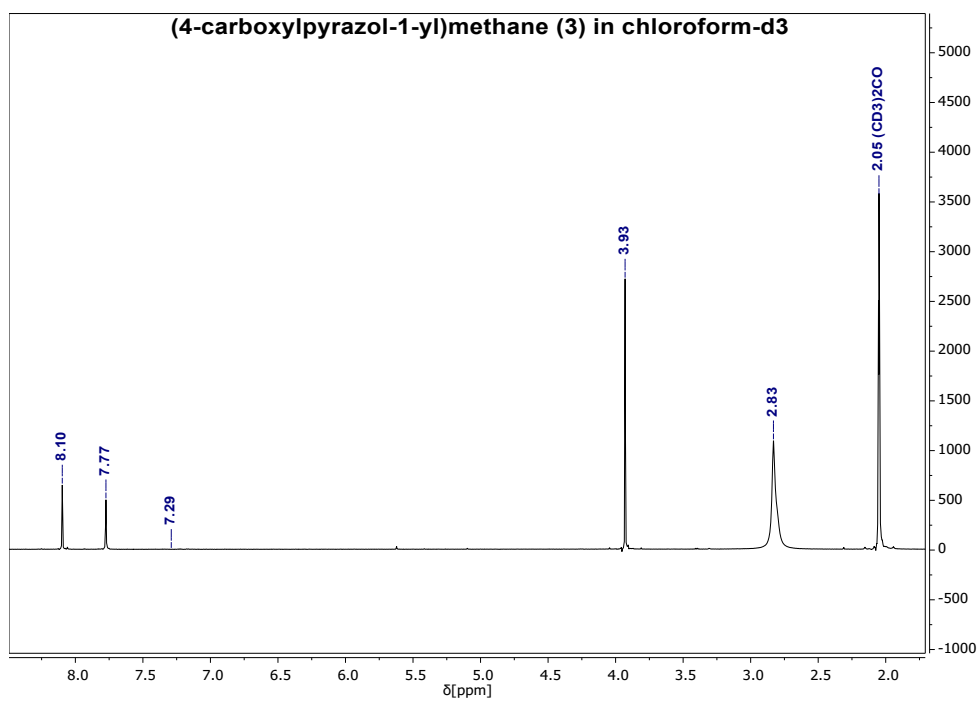


Figure S4.  $^1\text{H}$  NMR spectrum of (4-carboxypyrazol-1-yl)methane (**3**) in chloroform-d<sub>3</sub>.

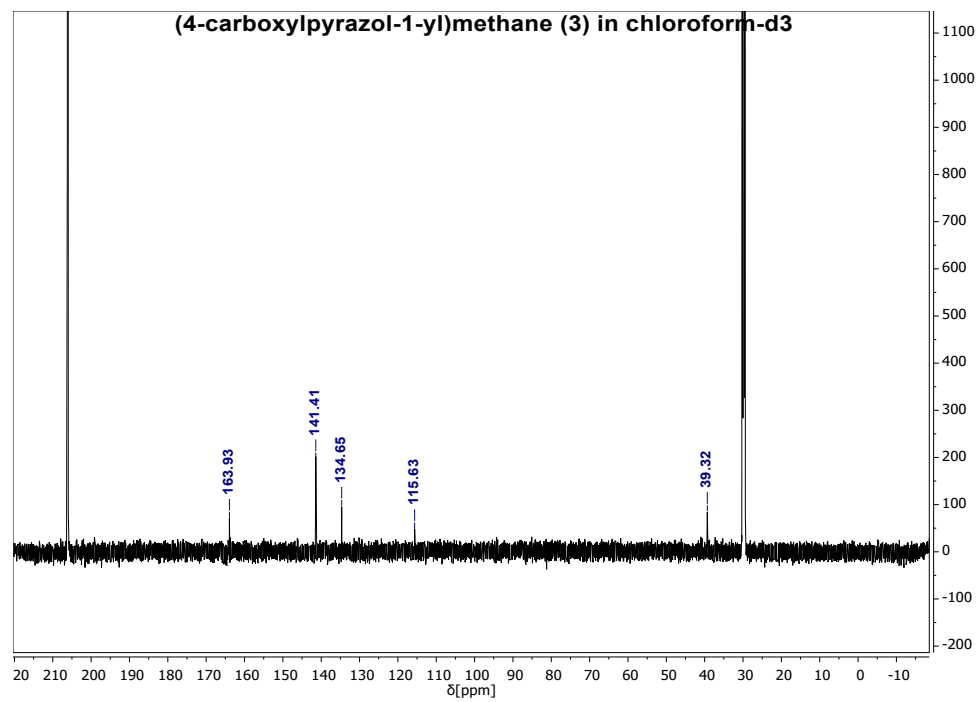


Figure S5. <sup>13</sup>C NMR spectrum of (4-carboxypyrazol-1-yl)methane (**3**) in chloroform-d<sub>3</sub>.



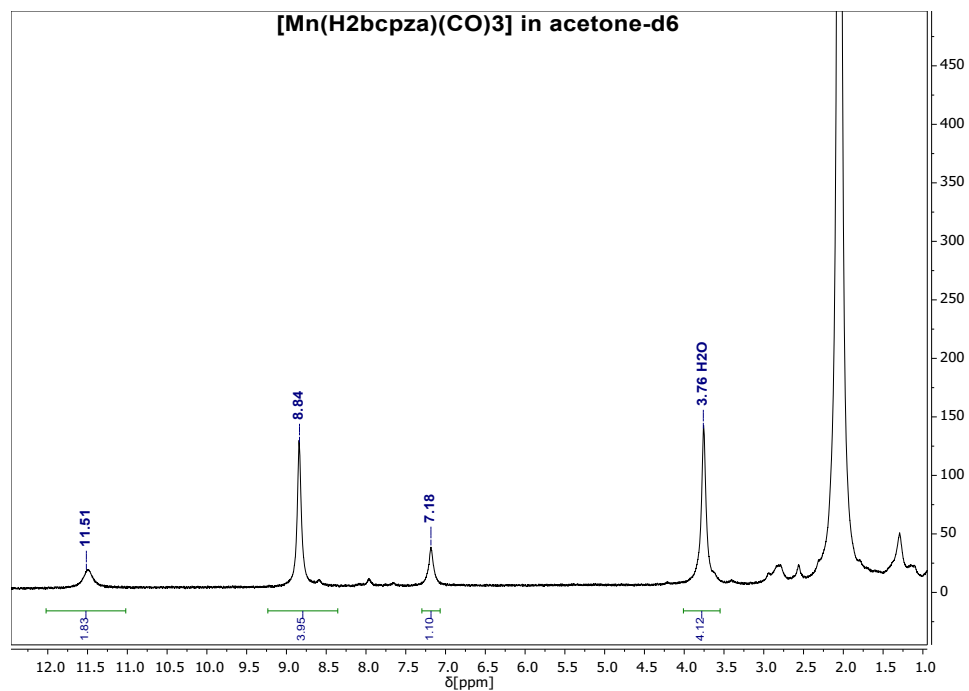


Figure S6. <sup>1</sup>H NMR spectrum of [Mn(H<sub>2</sub>bcpza)(CO)<sub>3</sub>] (**4**) in acetone-d<sub>6</sub>.

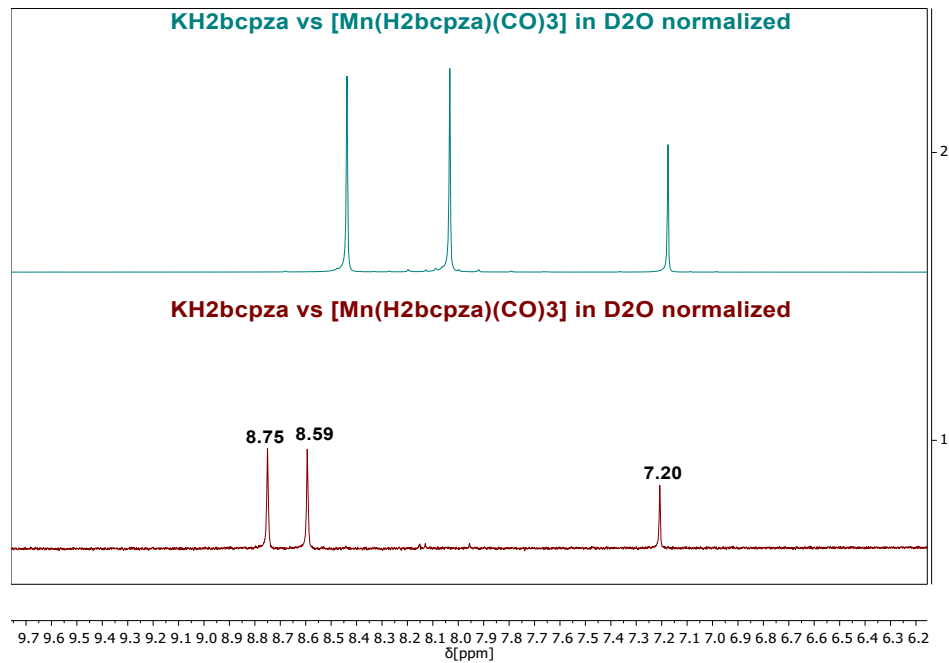
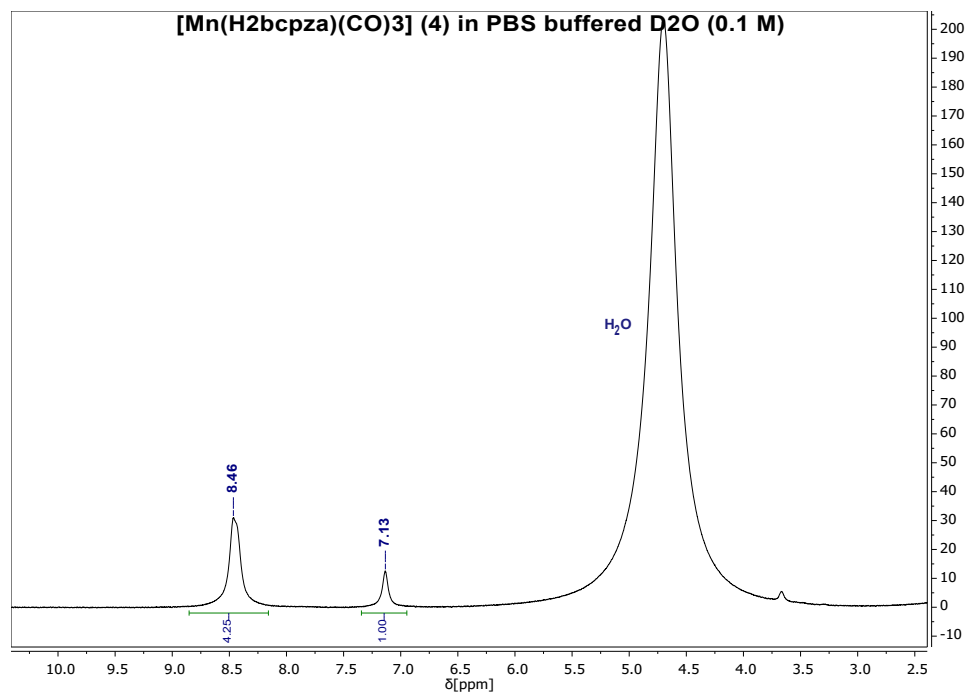
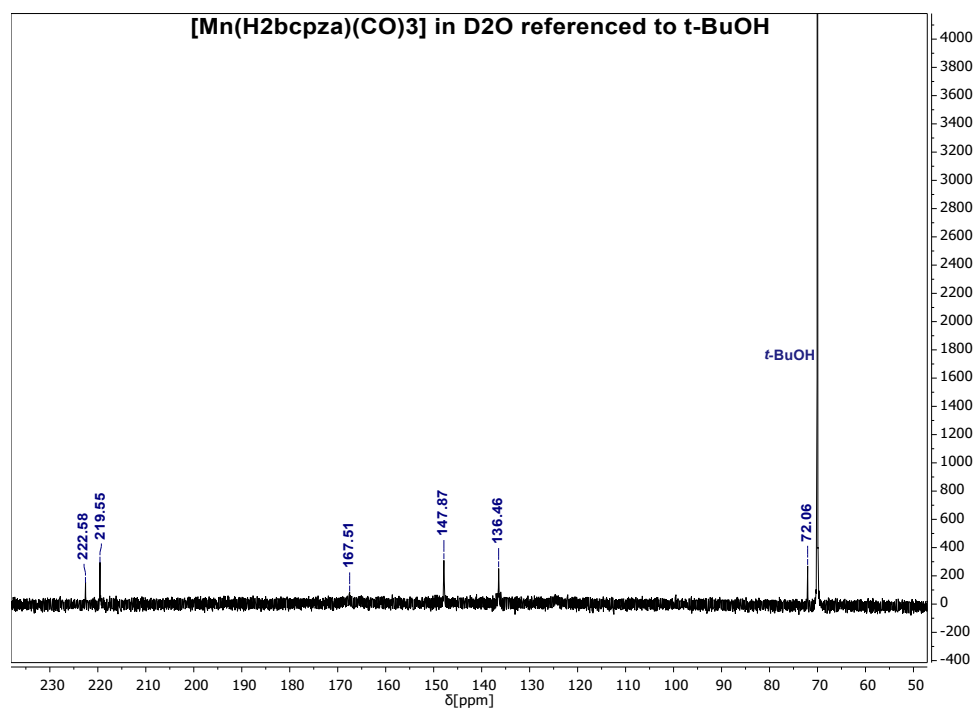


Figure S7. <sup>1</sup>H NMR of KH<sub>2</sub>bcpza in D<sub>2</sub>O (top) and [Mn(H<sub>2</sub>bcpza)(CO)<sub>3</sub>] (**4**) in D<sub>2</sub>O (bottom, normalized).



**Figure S8.** <sup>1</sup>H NMR spectrum of [Mn(H<sub>2</sub>bcpza)(CO)<sub>3</sub>] (**4**) in PBS buffered D<sub>2</sub>O (0.1 M).



**Figure S9.** <sup>13</sup>C NMR spectrum of [Mn(H<sub>2</sub>bcpza)(CO)<sub>3</sub>] (**4**) in PBS buffered (0.1 M) D<sub>2</sub>O referenced to *t*-BuOH. The second carboxyl group as well as the quaternary carbon atom C<sup>4</sup><sub>pz</sub> could not be resolved.

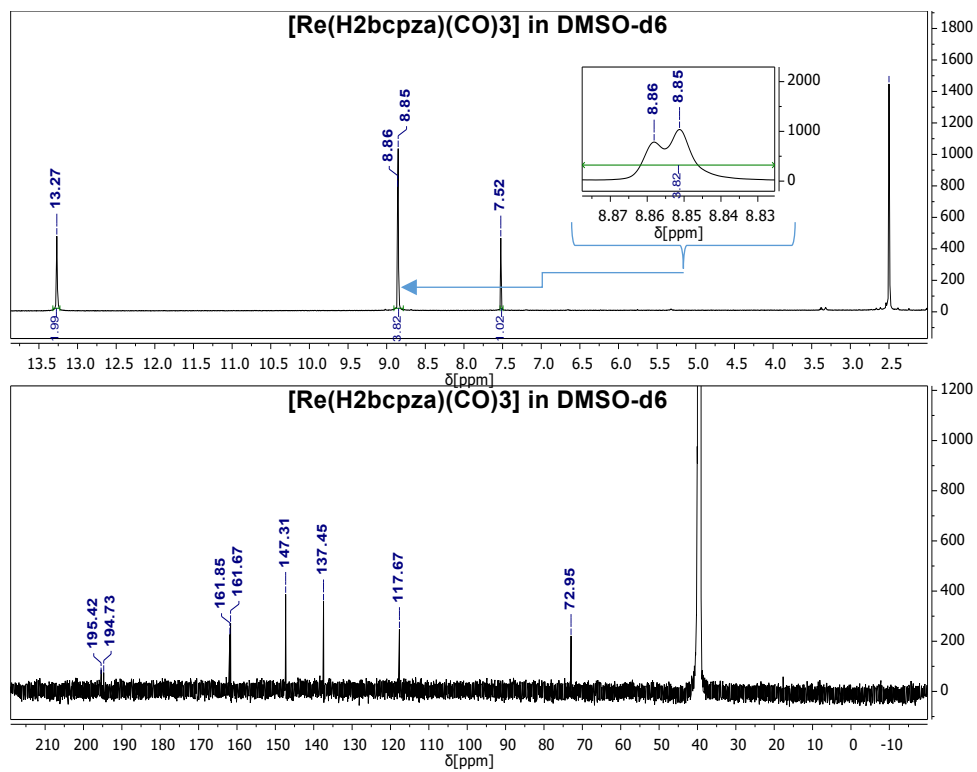


Figure S10.  $^1\text{H}$  &  $^{13}\text{C}$  NMR spectrum of  $[\text{Re}(\text{H}_2\text{bcpza})(\text{CO})_3]$  (5) in  $\text{dmsO-d}_6$ .

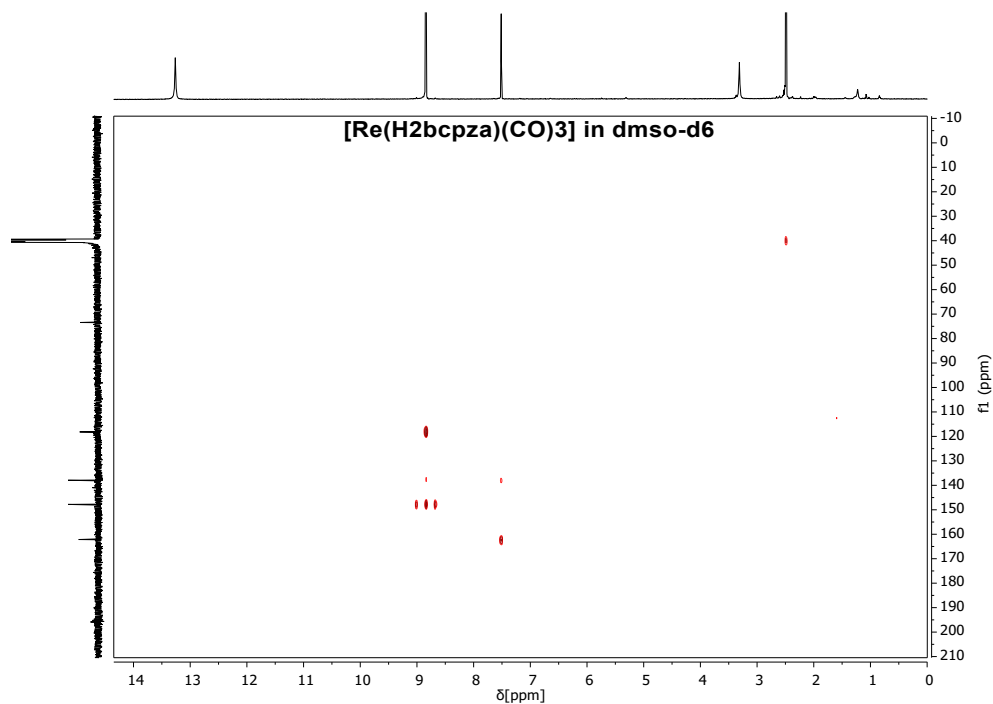


Figure S11. 2D HMBC spectrum of  $[\text{Re}(\text{H}_2\text{bcpza})(\text{CO})_3]$  (5) in  $\text{dmsO-d}_6$ .

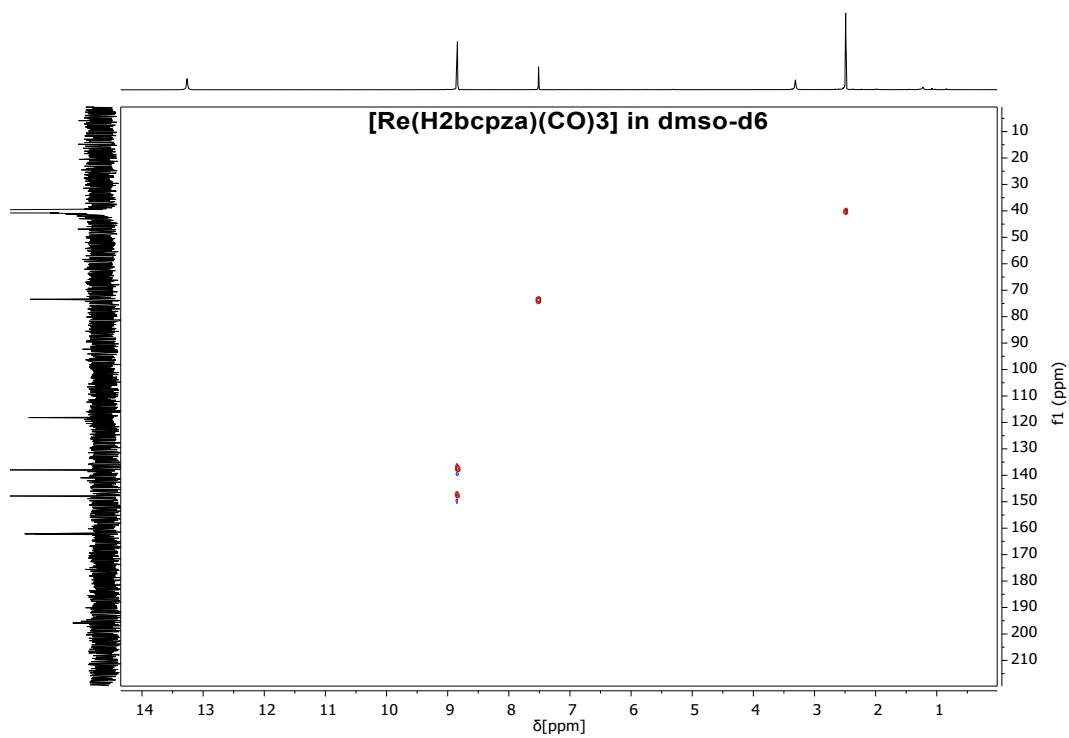


Figure S12. 2D HSQC spectrum of  $[\text{Re}(\text{H}_2\text{bcpza})(\text{CO})_3]$  (**5**) in  $\text{dms0-d}_6$ .

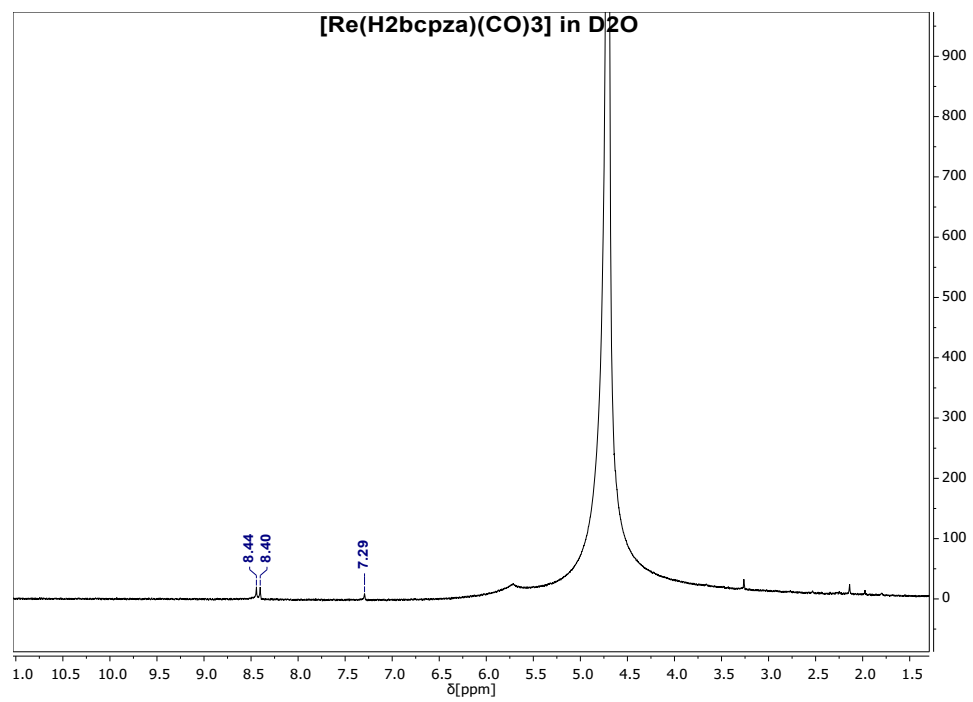


Figure S13.  $^1\text{H}$  NMR spectrum of  $[\text{Re}(\text{H}_2\text{bcpza})(\text{CO})_3]$  (**5**) in  $\text{D}_2\text{O}$ .

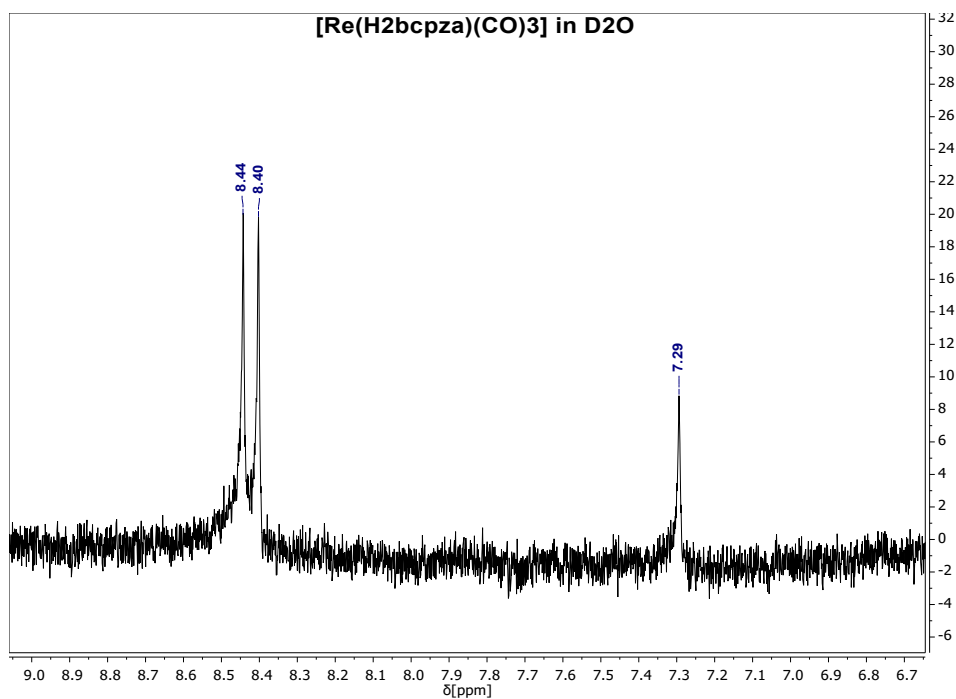


Figure S14. <sup>1</sup>H NMR spectrum of [Re(H<sub>2</sub>bcpza)(CO)<sub>3</sub>] (5) in D<sub>2</sub>O.

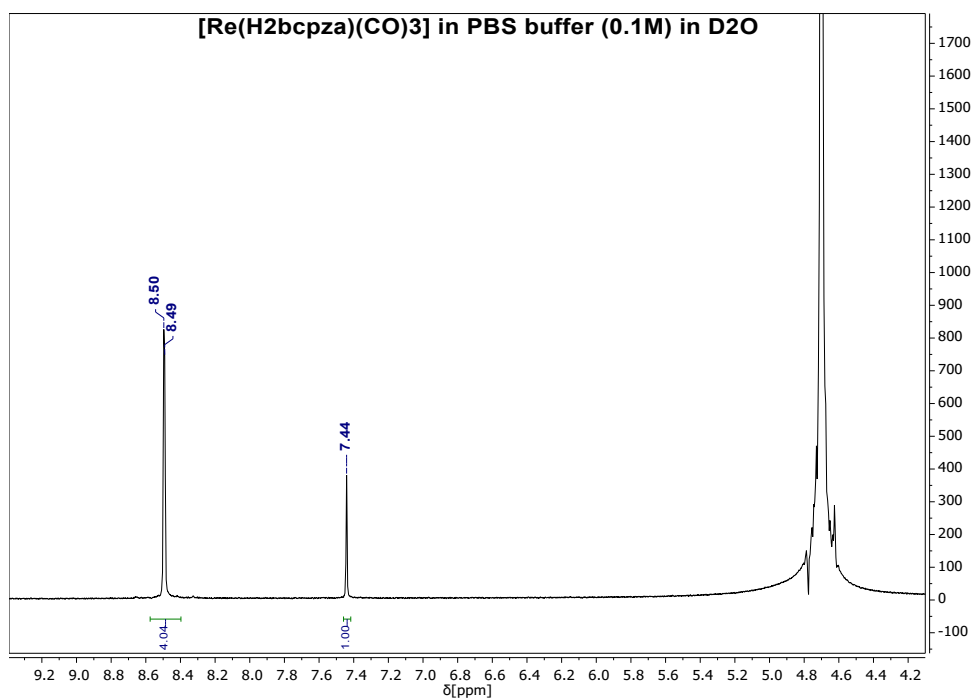
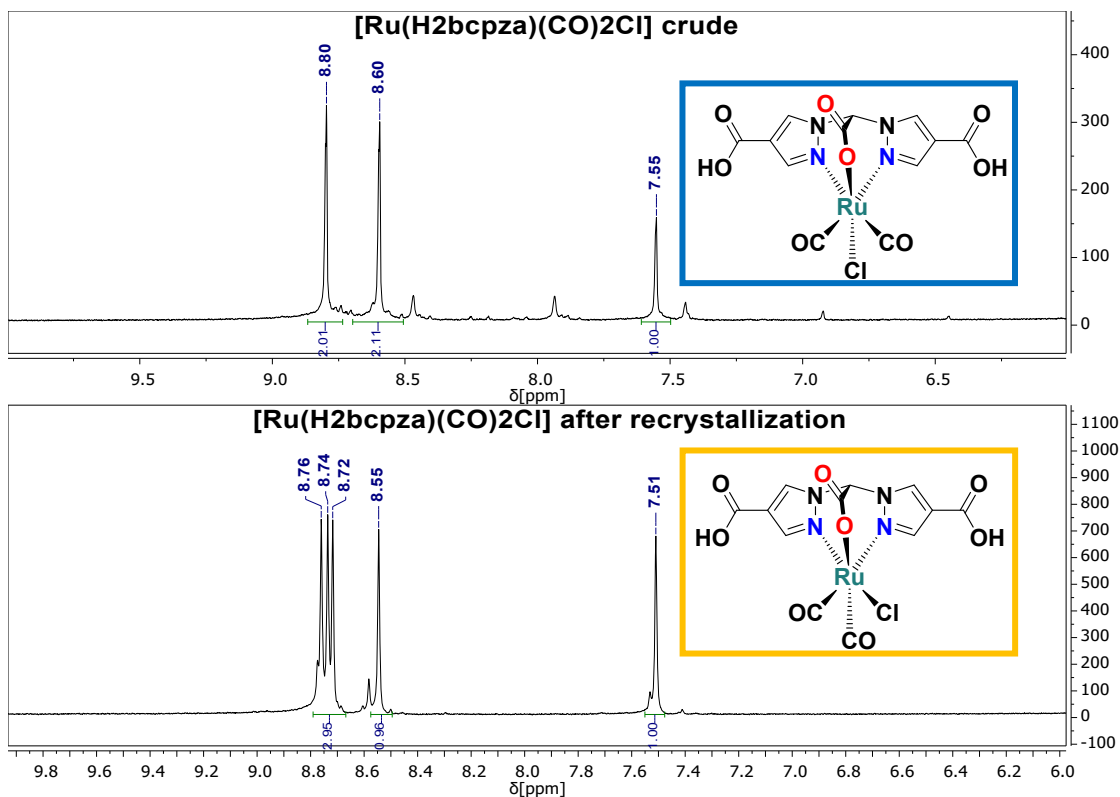


Figure S15. <sup>13</sup>C NMR spectrum of [Re(H<sub>2</sub>bcpza)(CO)<sub>3</sub>] (5) in PBS buffered (0.1M) D<sub>2</sub>O.



**Figure S16.** Top:  $^1\text{H}$  NMR spectrum of the crude product  $[\text{Ru}(\text{H}_2\text{bcpza})\text{Cl}(\text{CO})_2]$  obtained by removing the solvent of the reaction mixture. The spectrum was recorded in methanol- $\text{d}_4$  and mainly displays the symmetric isomer  $[\text{Ru}(\text{H}_2\text{bcpza})\text{Cl}(\text{CO})_2]$  (**6a**). Bottom:  $^1\text{H}$  NMR spectrum of the asymmetric  $[\text{Ru}(\text{H}_2\text{bcpza})\text{Cl}(\text{CO})_2]$  (**6b**) obtained after purification of **6a** and subsequent recrystallization from methanol. The spectrum was recorded in methanol- $\text{d}_4$ .

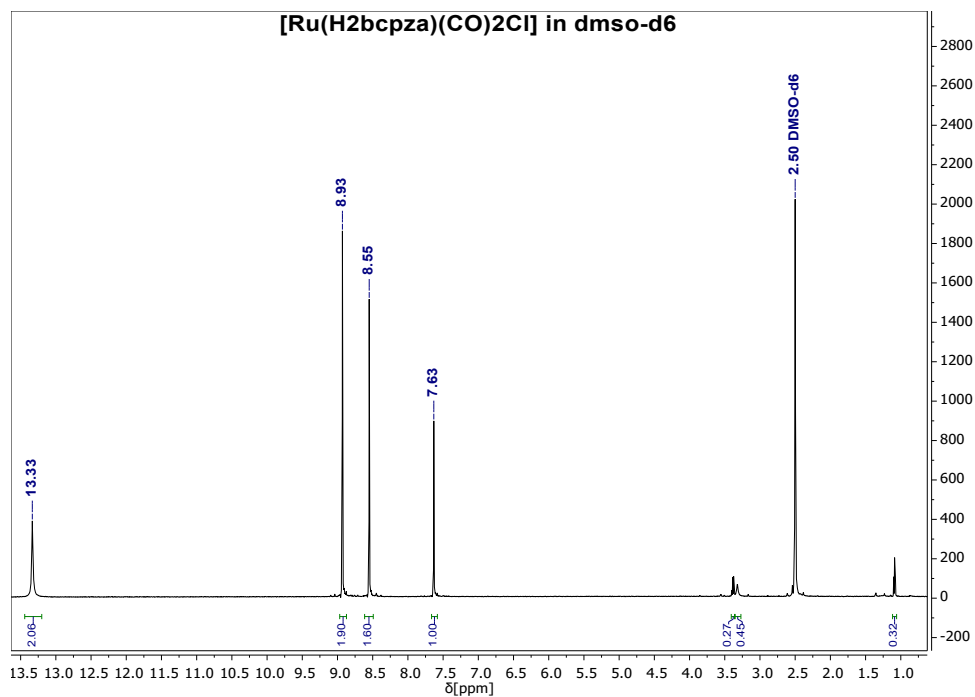


Figure S17. <sup>1</sup>H NMR spectrum of [Ru(H<sub>2</sub>bcpza)Cl(CO)<sub>2</sub>] (6a) in dms0-d<sub>6</sub>.

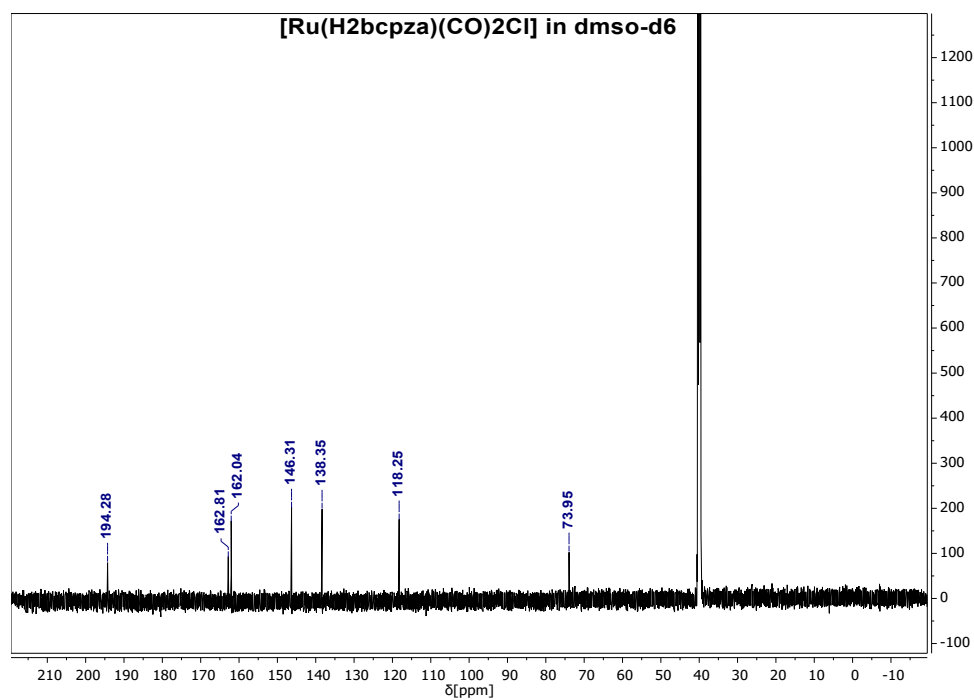


Figure S18. <sup>13</sup>C NMR spectrum of [Ru(H<sub>2</sub>bcpza)Cl(CO)<sub>2</sub>] (6a) in dms0-d<sub>6</sub>.

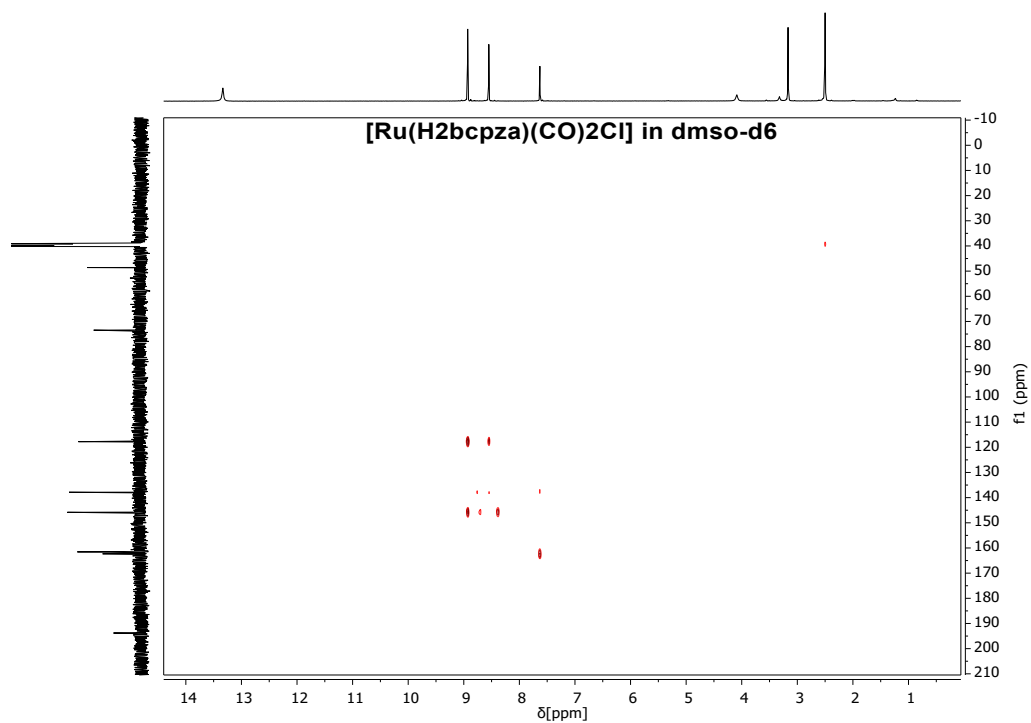


Figure S19. 2D HMBC spectrum of  $[\text{Ru}(\text{H}_2\text{bcpza})\text{Cl}(\text{CO})_2]$  (**6a**) in  $\text{dms0-d}_6$ .

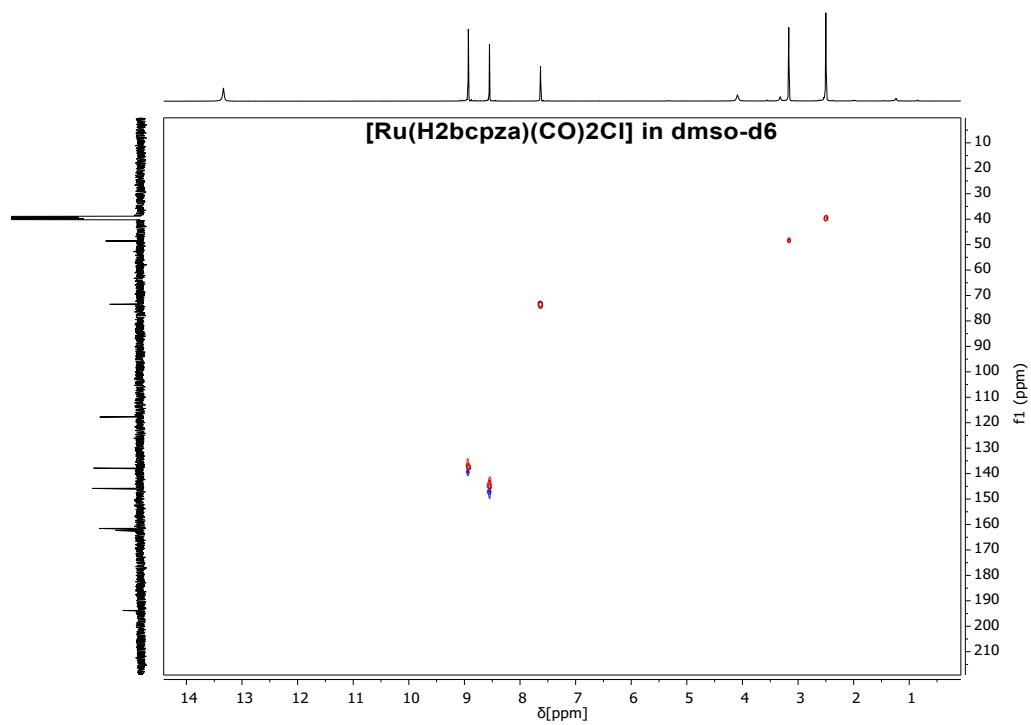


Figure S20. 2D HSQC spectrum of  $[\text{Ru}(\text{H}_2\text{bcpza})\text{Cl}(\text{CO})_2]$  (**6a**) in  $\text{dms0-d}_6$ .



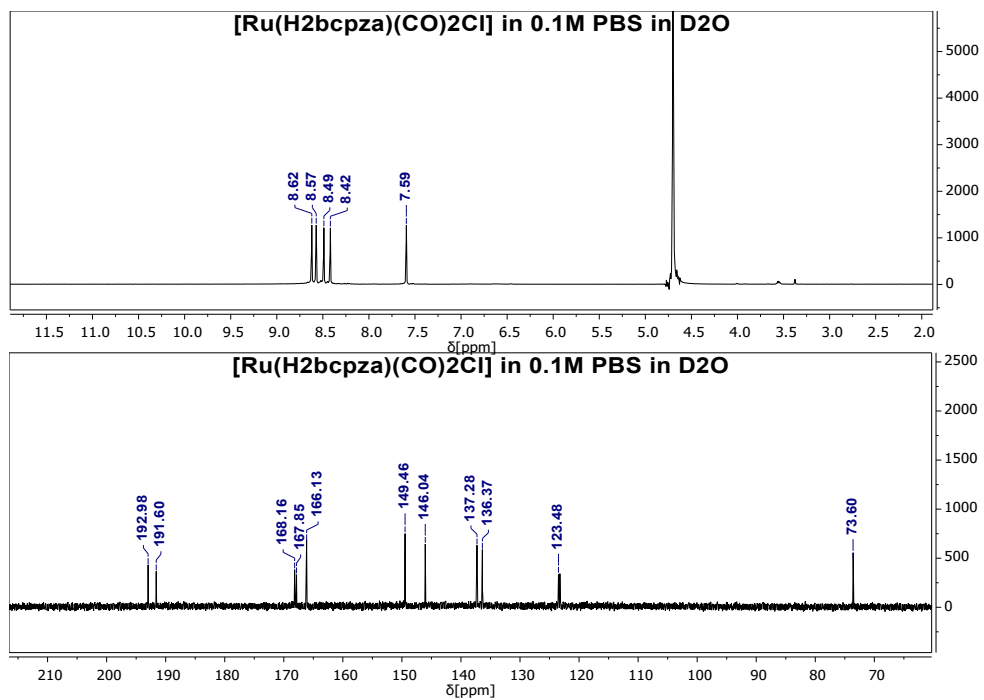


Figure S21.  $^1\text{H}$  &  $^{13}\text{C}$  NMR spectrum of  $[\text{Ru}(\text{H}_2\text{bcpza})\text{Cl}(\text{CO})_2]$  (**6b**) in PBS buffer (0.1 M) in  $\text{D}_2\text{O}$ .

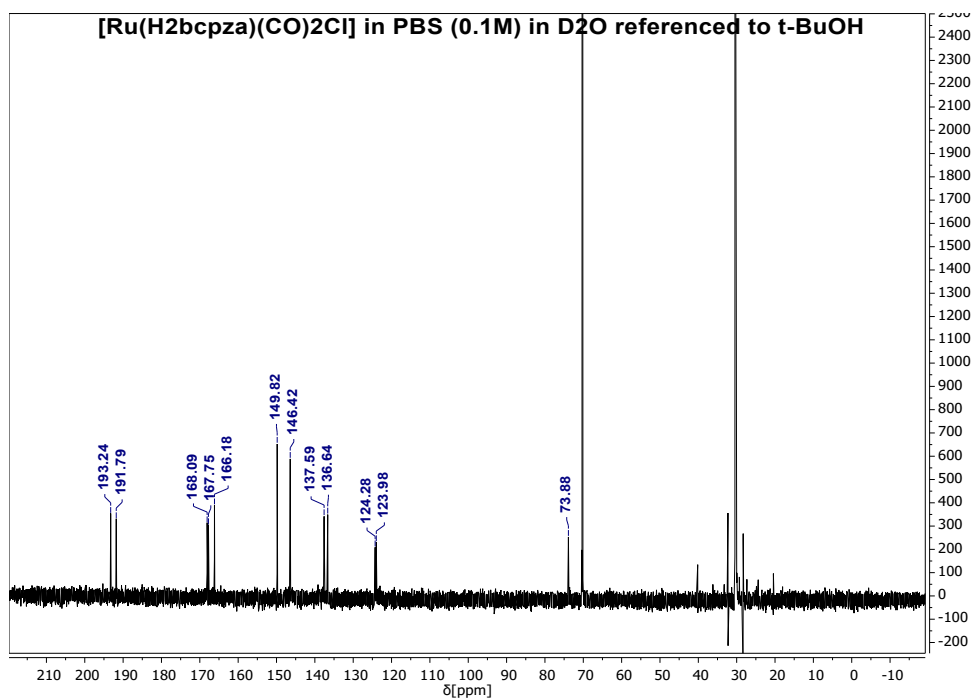


Figure S22.  $^{13}\text{C}$  NMR spectrum of  $[\text{Ru}(\text{H}_2\text{bcpza})\text{Cl}(\text{CO})_2]$  (**6b**) in PBS buffer (0.1 M) in  $\text{D}_2\text{O}$  referenced to  $t\text{-BuOH}$ .

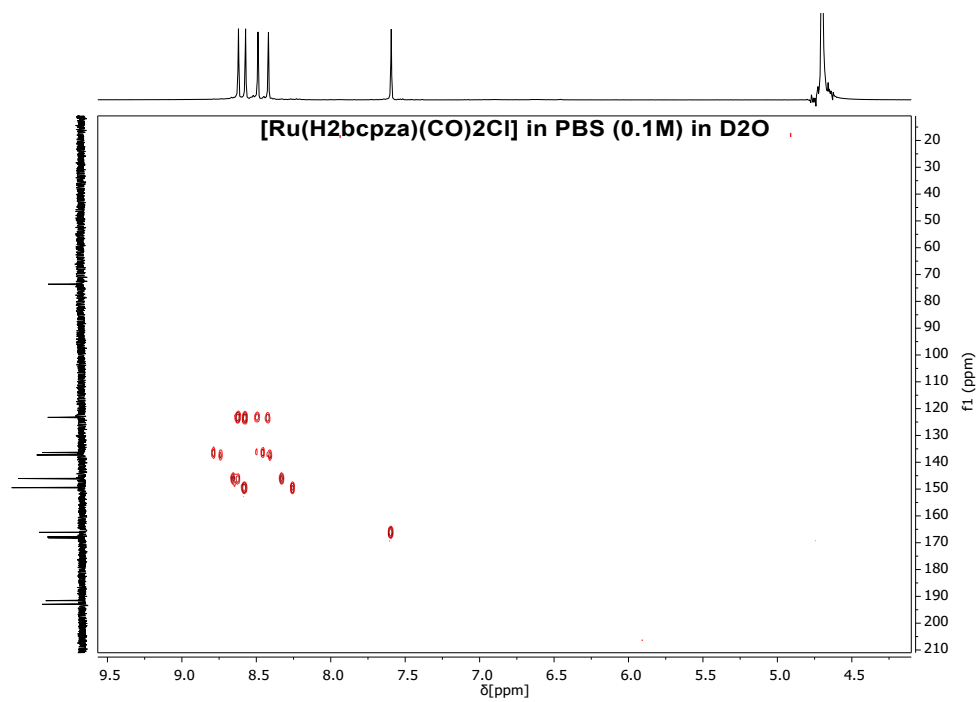


Figure S23. 2D HMBC spectrum of  $[\text{Ru}(\text{H}_2\text{bcpza})\text{Cl}(\text{CO})_2]$  (**6b**) in PBS buffer (0.1 M) in  $\text{D}_2\text{O}$ .

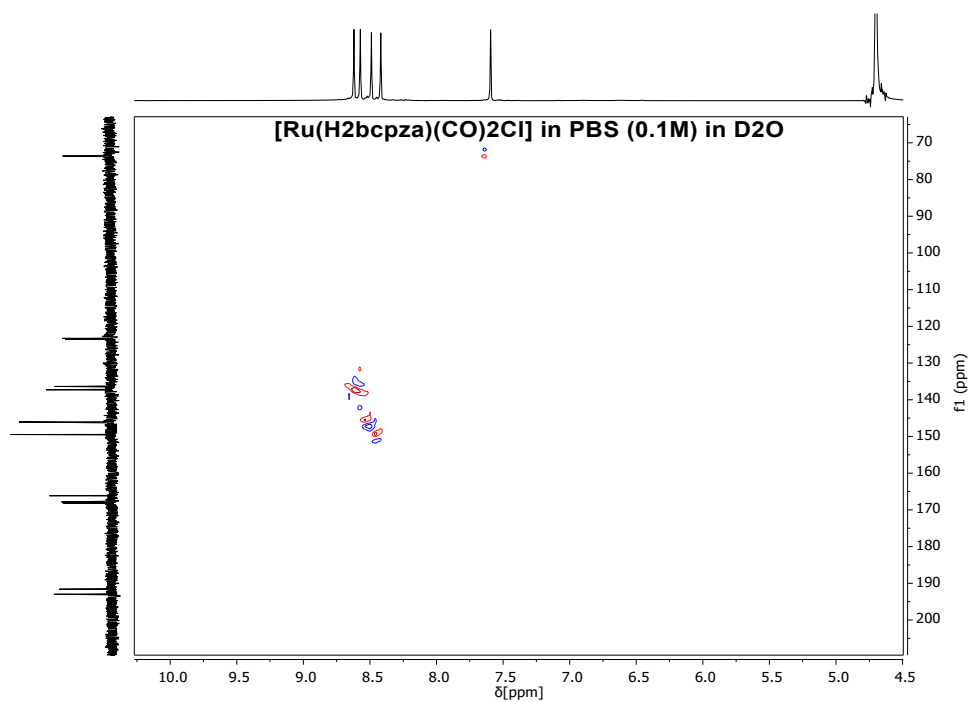
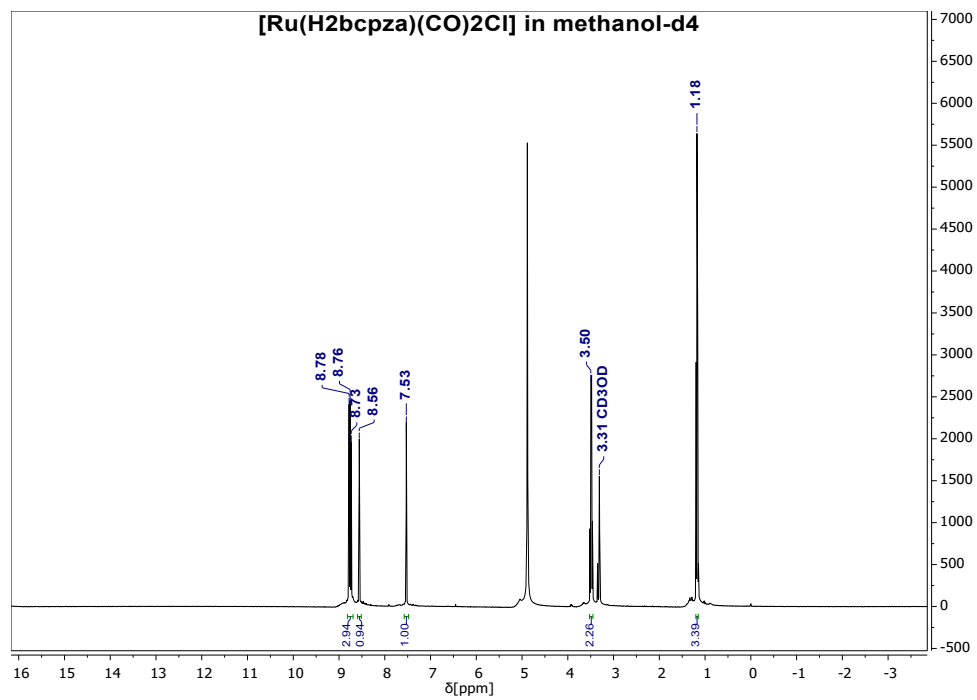
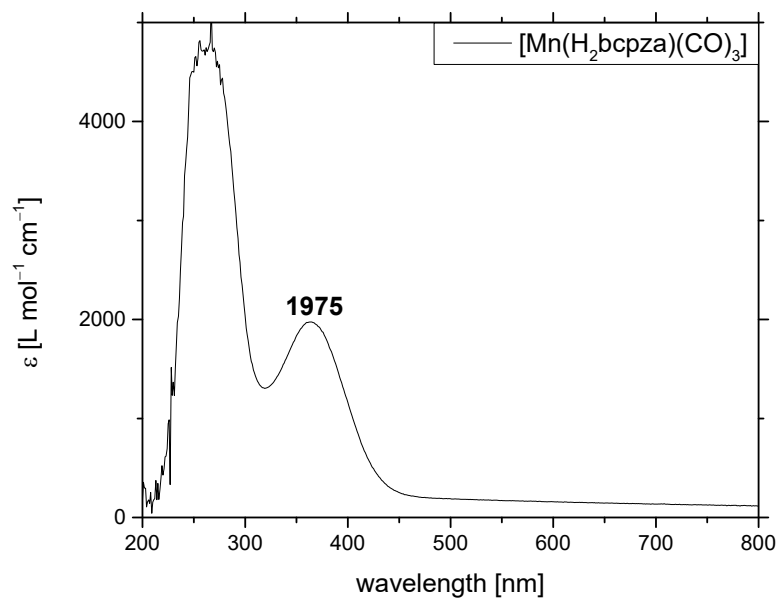


Figure S24. 2D HSQC spectrum of  $[\text{Ru}(\text{H}_2\text{bcpza})\text{Cl}(\text{CO})_2]$  (**6b**) in PBS buffer (0.1 M) in  $\text{D}_2\text{O}$ .



**Figure S25.** <sup>1</sup>H NMR spectrum of [Ru(H<sub>2</sub>bcpza)Cl(CO)<sub>2</sub>] (**6b**) in methanol-d<sub>4</sub>.

### 3. UV-vis spectra



**Figure S26.** UV-vis spectrum of  $[\text{Mn}(\text{H}_2\text{bcpza})(\text{CO})_3]$  (**4**) (0.536 mM) in PBS buffer (0.1 M) with  $\epsilon_{363} = 1975 \text{ L mol}^{-1} \text{cm}^{-1}$ .

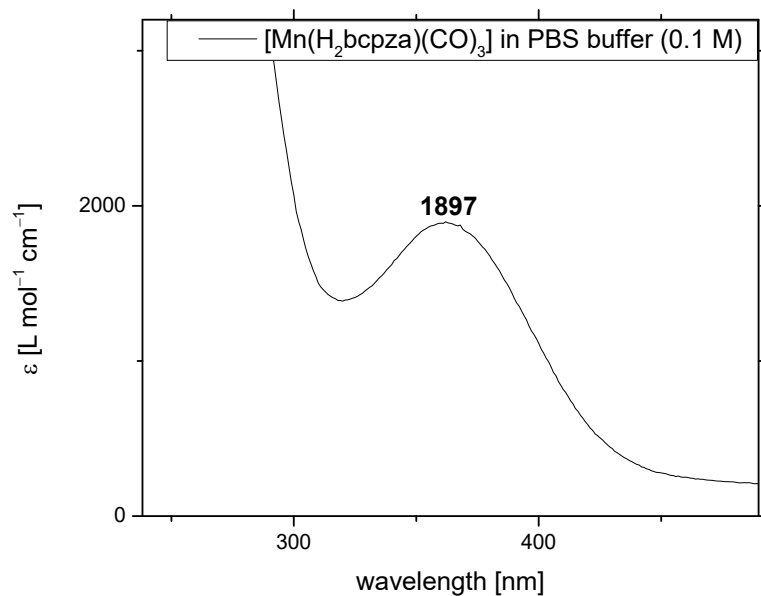


**Figure S27.** UV-vis spectrum of  $[\text{Mn}(\text{H}_2\text{bcpza})(\text{CO})_3]$  (**4**) (0.383 mM) in PBS buffer (0.1 M) with  $\epsilon_{363} = 1897 \text{ L mol}^{-1} \text{cm}^{-1}$ .

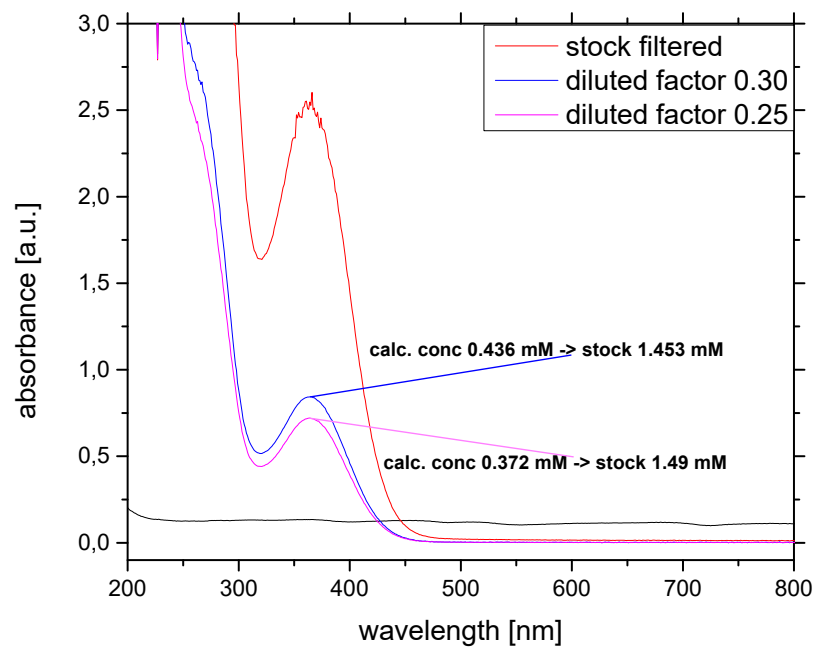


**Figure S28.** UV-vis spectrum of [Mn(H<sub>2</sub>bcpza)(CO)<sub>3</sub>] (4) in H<sub>2</sub>O with different dilutions of stock solution.

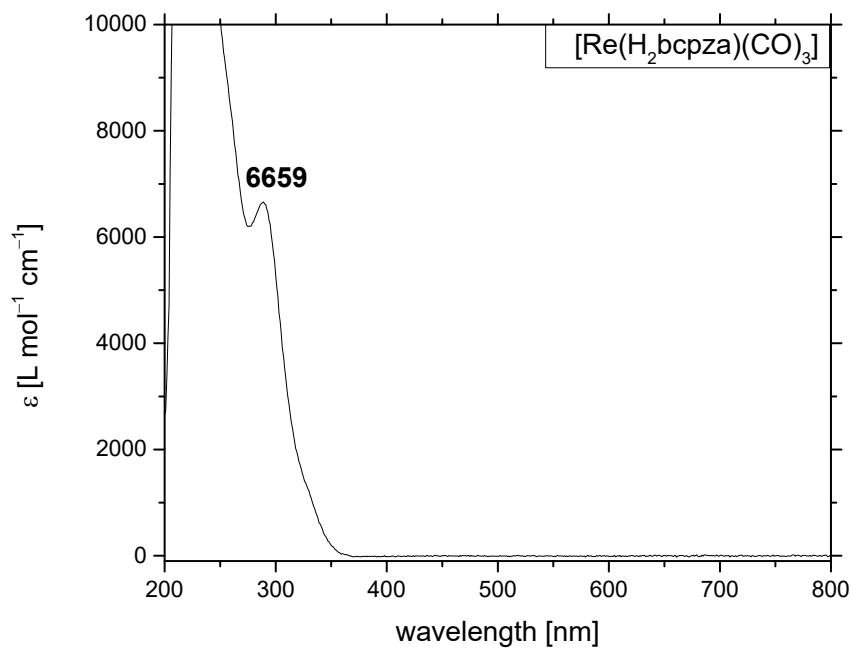


**Figure S29.** UV-vis spectrum of [Re(H<sub>2</sub>bcpza)(CO)<sub>3</sub>] (5) (0.0837 mM) in methanol.

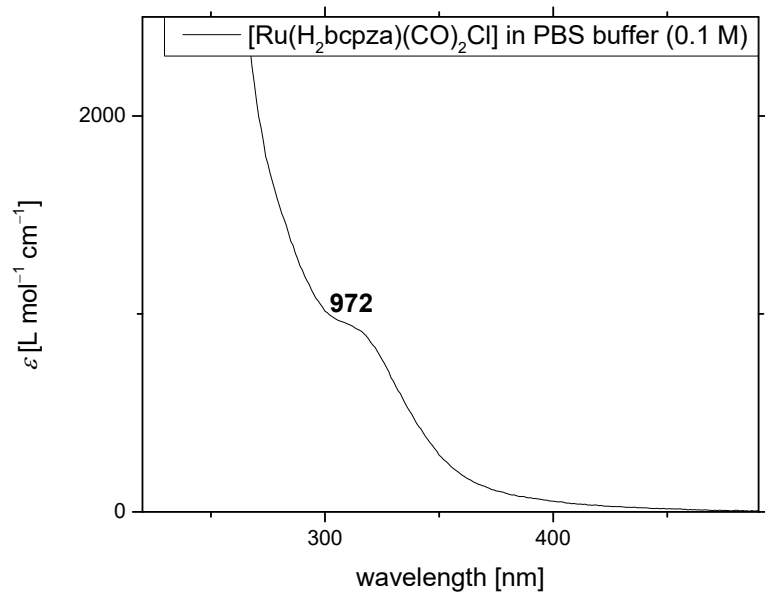


**Figure S30.** UV-vis spectrum of  $[\text{Ru}(\text{H}_2\text{bcpza})\text{Cl}(\text{CO})_2]$  (**6b**) (PBS 0.1 M).  $\lambda_{\text{max}}$  ( $\epsilon$  [ $\text{L mol}^{-1} \text{cm}^{-1}$ ]) = 310 (972) nm.

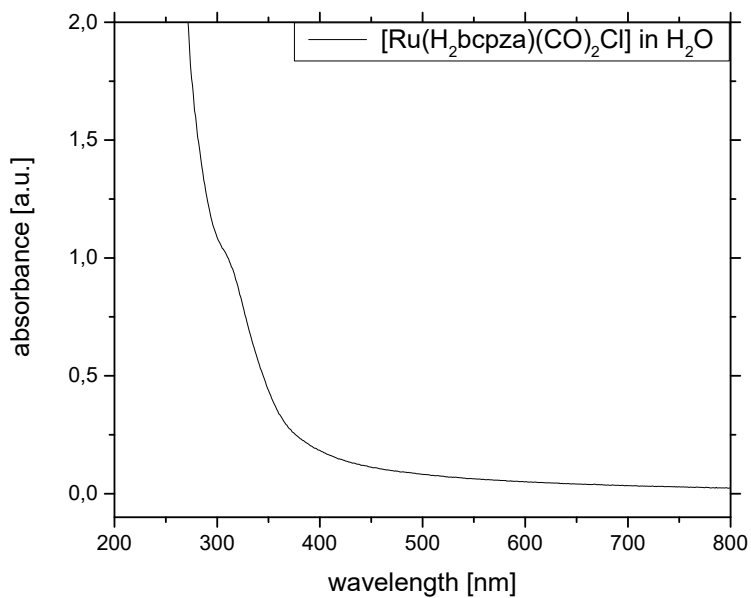


**Figure S31.** UV-vis spectrum of a saturated solution of  $[\text{Ru}(\text{H}_2\text{bcpza})\text{Cl}(\text{CO})_2]$  (**6b**) in  $\text{H}_2\text{O}$ . Concentration according to Beer-Lambert law was calculated to 1.03 mmol.

#### 4. IR spectra

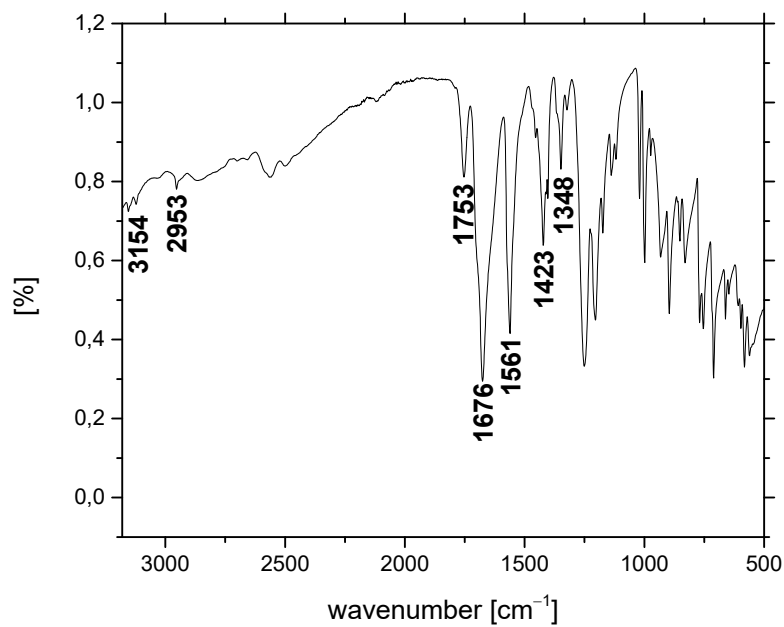


Figure S32. IR(ATR) spectrum of H<sub>3</sub>bcpza (2).

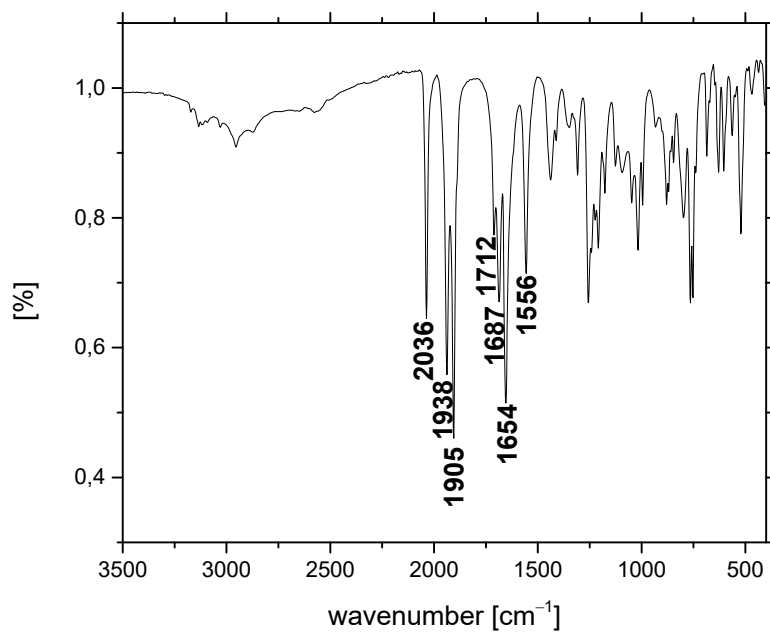
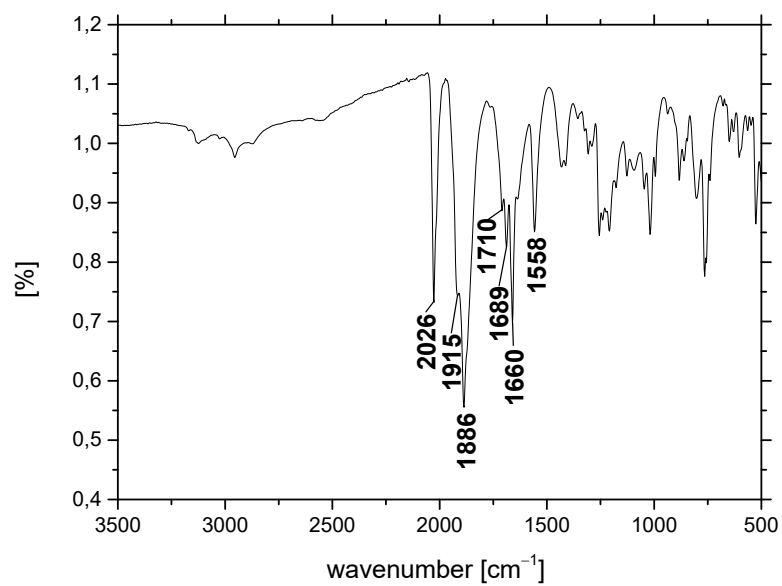
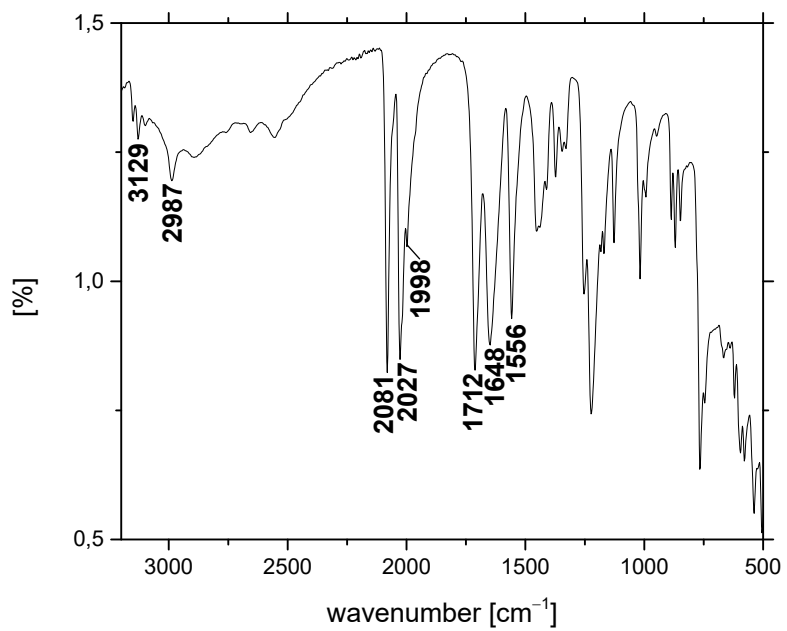


Figure S33. IR (ATR) spectrum of [Mn(H<sub>2</sub>bcpza)(CO)<sub>3</sub>] (4).



**Figure S34.** IR (ATR) spectrum of  $[\text{Re}(\text{H}_2\text{bcpza})(\text{CO})_3]$  (**5**).



**Figure S35.** IR spectrum of crystals grown from crude aqueous phase of **6a/6b** after washing process.



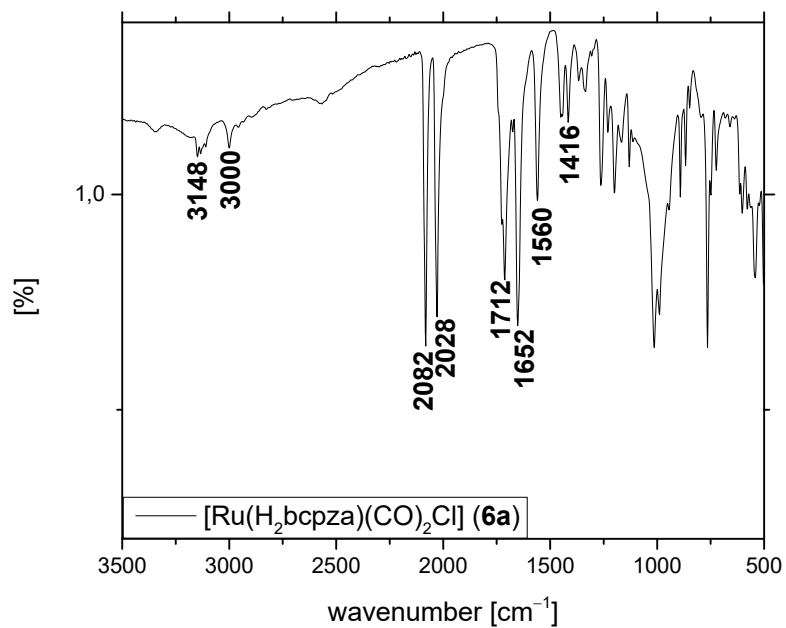


Figure S36. IR(ATR) spectrum of [Ru(H<sub>2</sub>bcpza)Cl(CO)<sub>2</sub>] (6a).

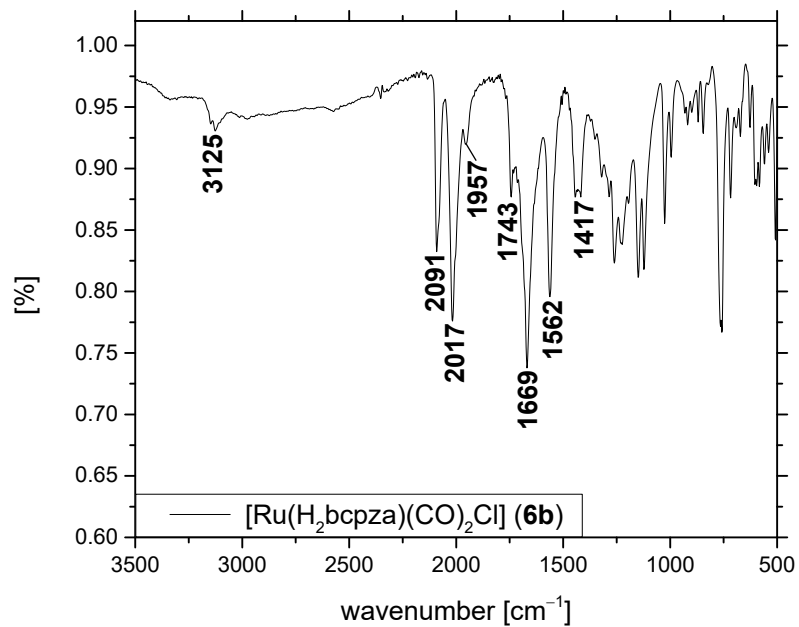
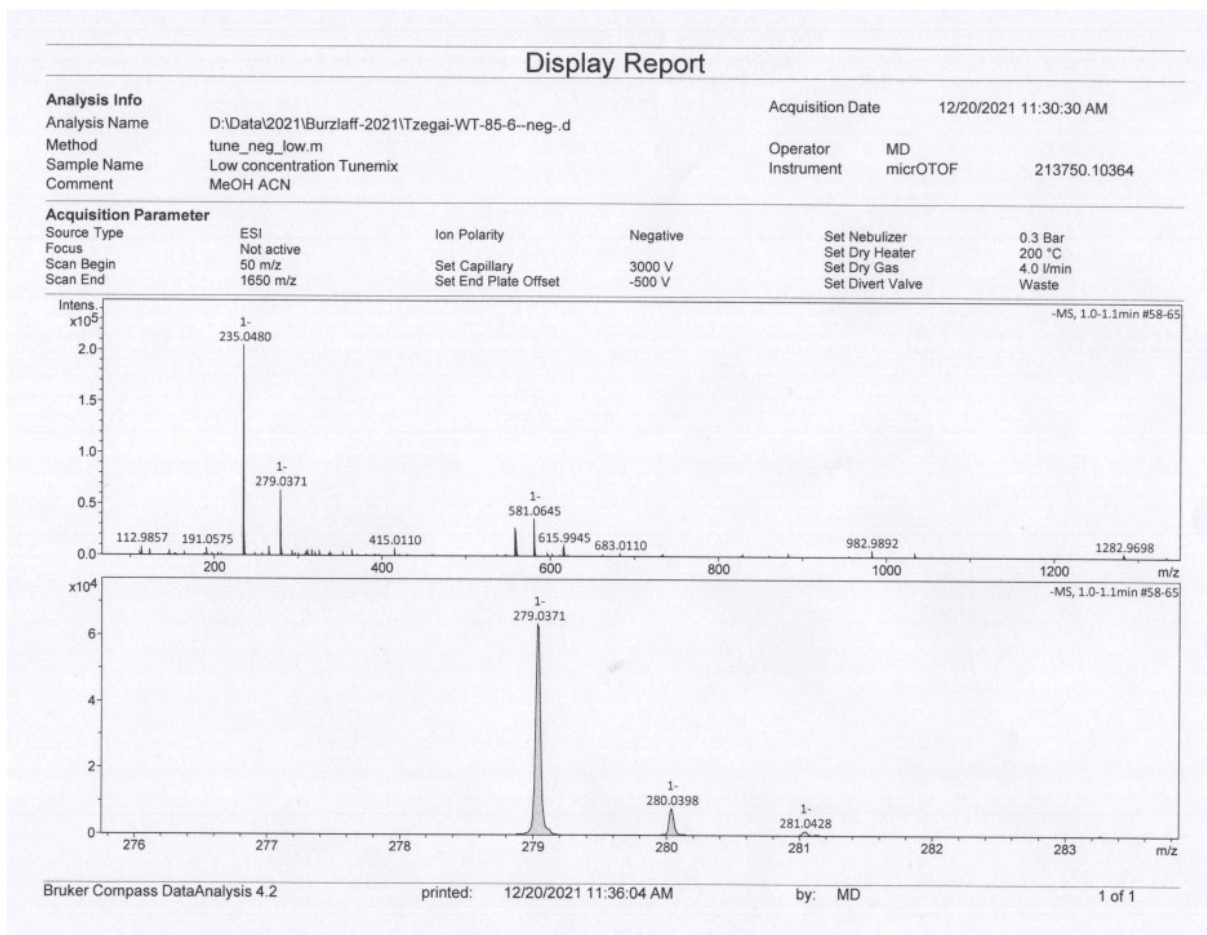


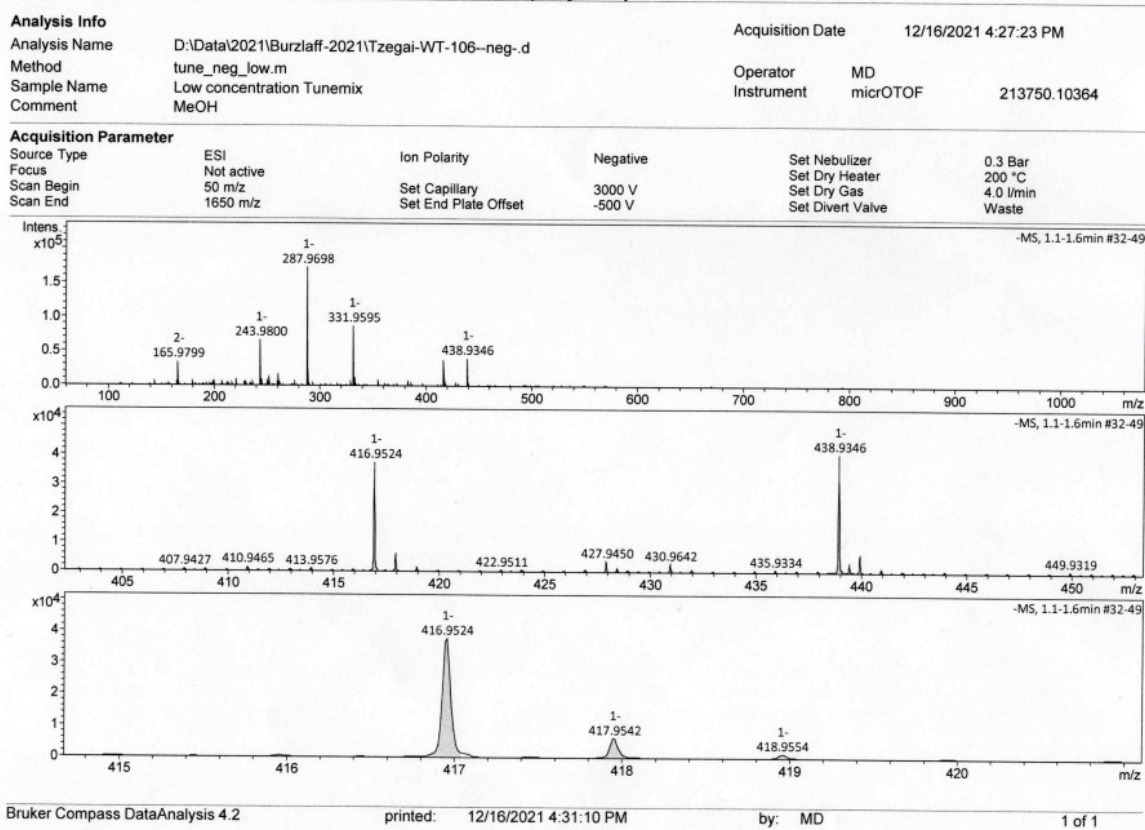
Figure S37. IR(ATR) spectrum of [Ru(H<sub>2</sub>bcpza)Cl(CO)<sub>2</sub>] (6b).

## 5. MS data

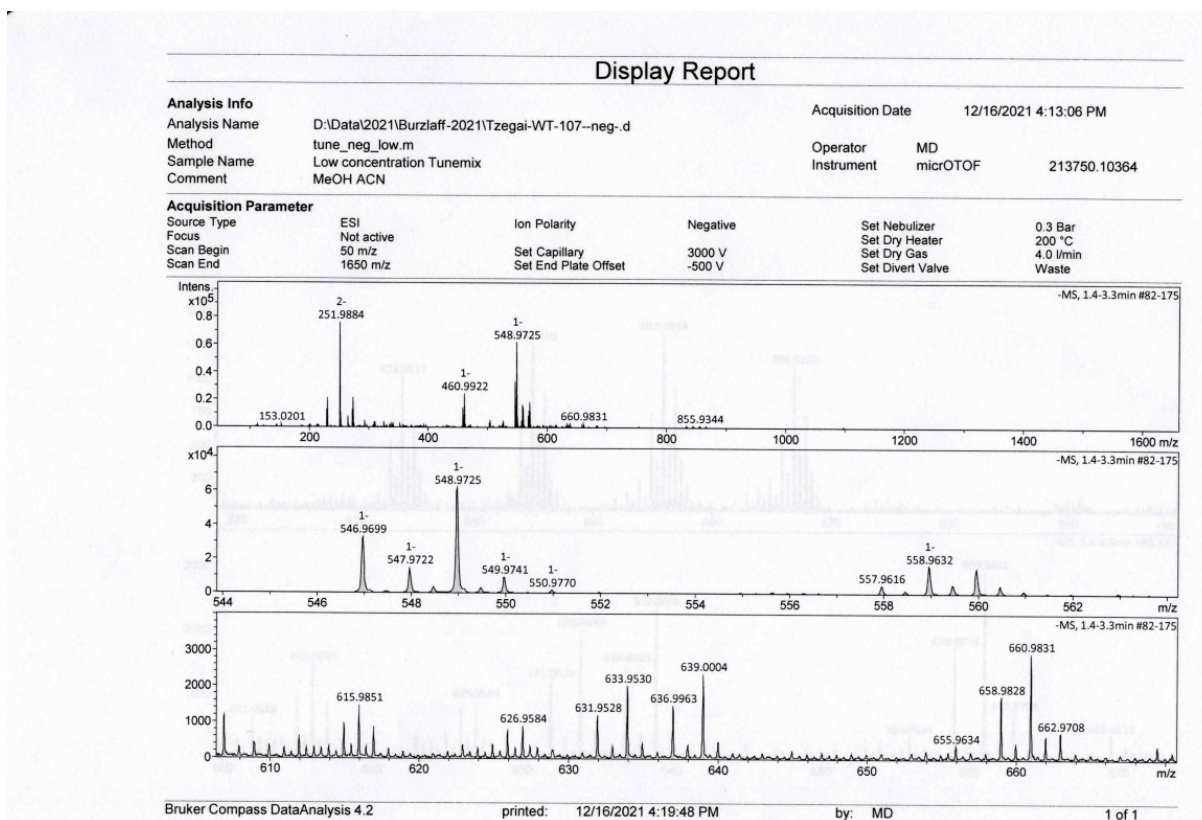


**Figure S38.** ESI-MS (negative ion mode) of H<sub>3</sub>bcpza (**2**) in methanol+acetonitrile.

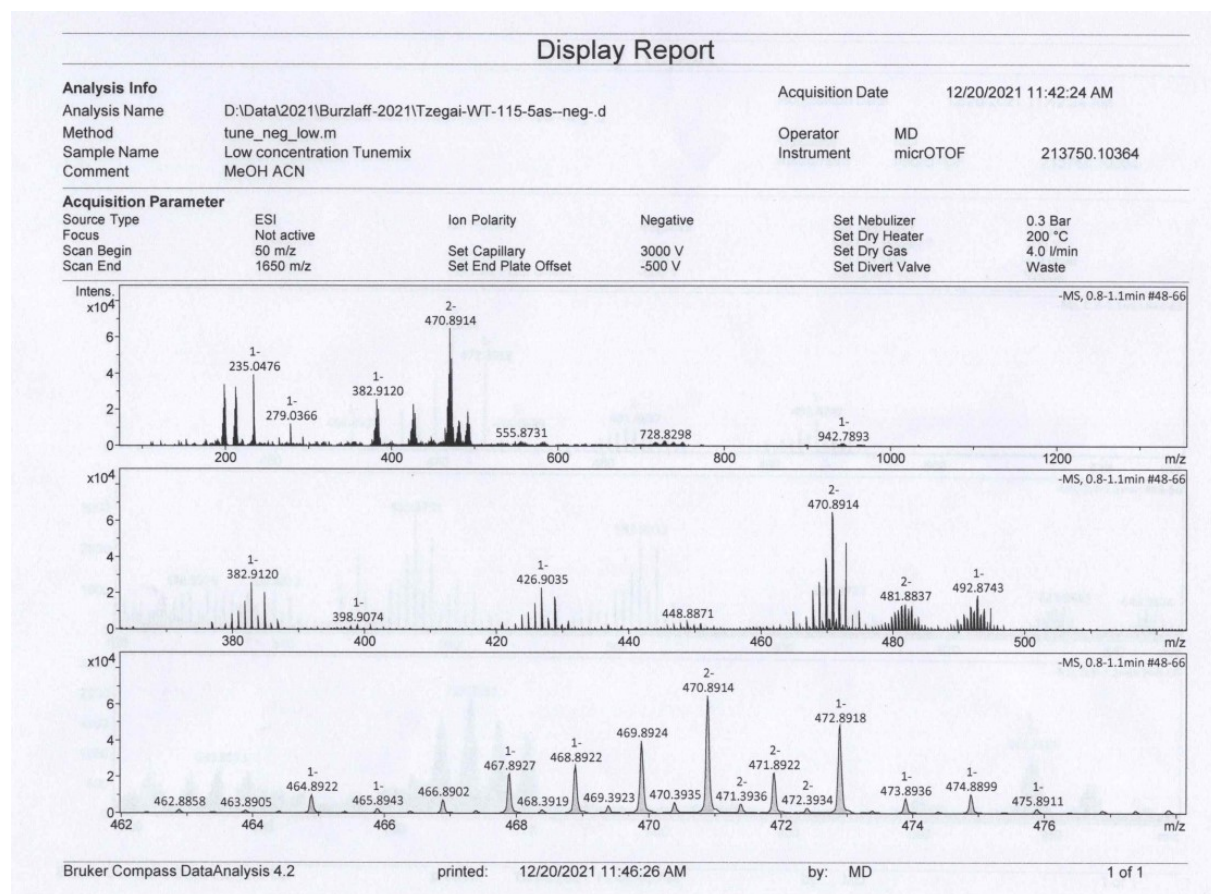
## Display Report



**Figure S39** ESI-MS (negative ion mode) spectrum of  $[\text{Mn}(\text{H}_2\text{bcpza})(\text{CO})_3]$  (**4**) in methanol.

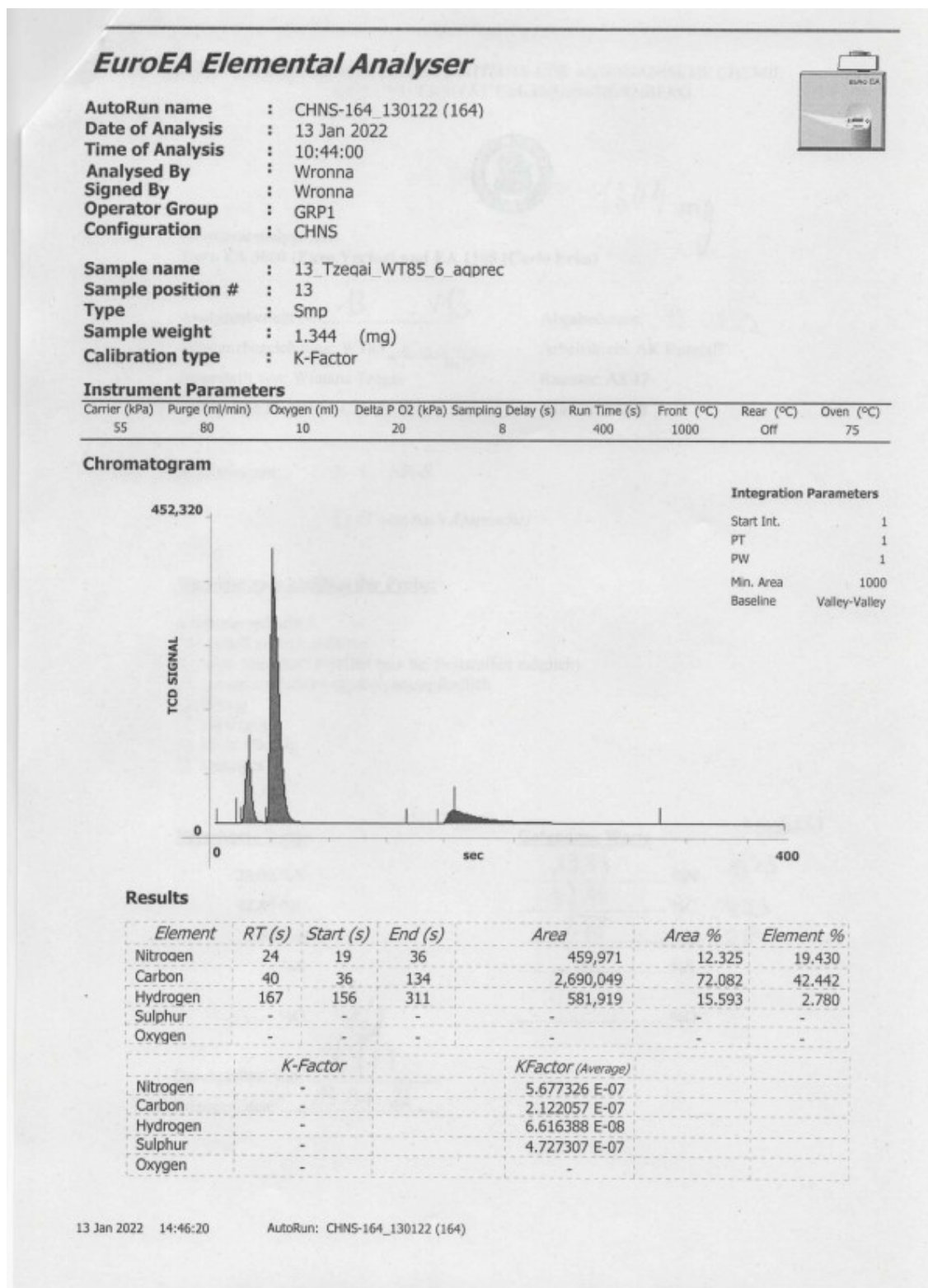


**Figure S40.** ESI-MS (negative ion mode) of  $[\text{Re}(\text{H}_2\text{bcpza})(\text{CO})_3]$  (**5**) recorded in methanol/acetonitrile.



**Figure S41.** ESI-MS (negative ion mode) of  $[\text{Ru}(\text{H}_2\text{bcpza})\text{Cl}(\text{CO})_2]$  (**6b**) recorded in methanol+acetonitrile.

## 6. Elemental analyses

Figure S42. Elemental analysis of H<sub>3</sub>bcpza (2).

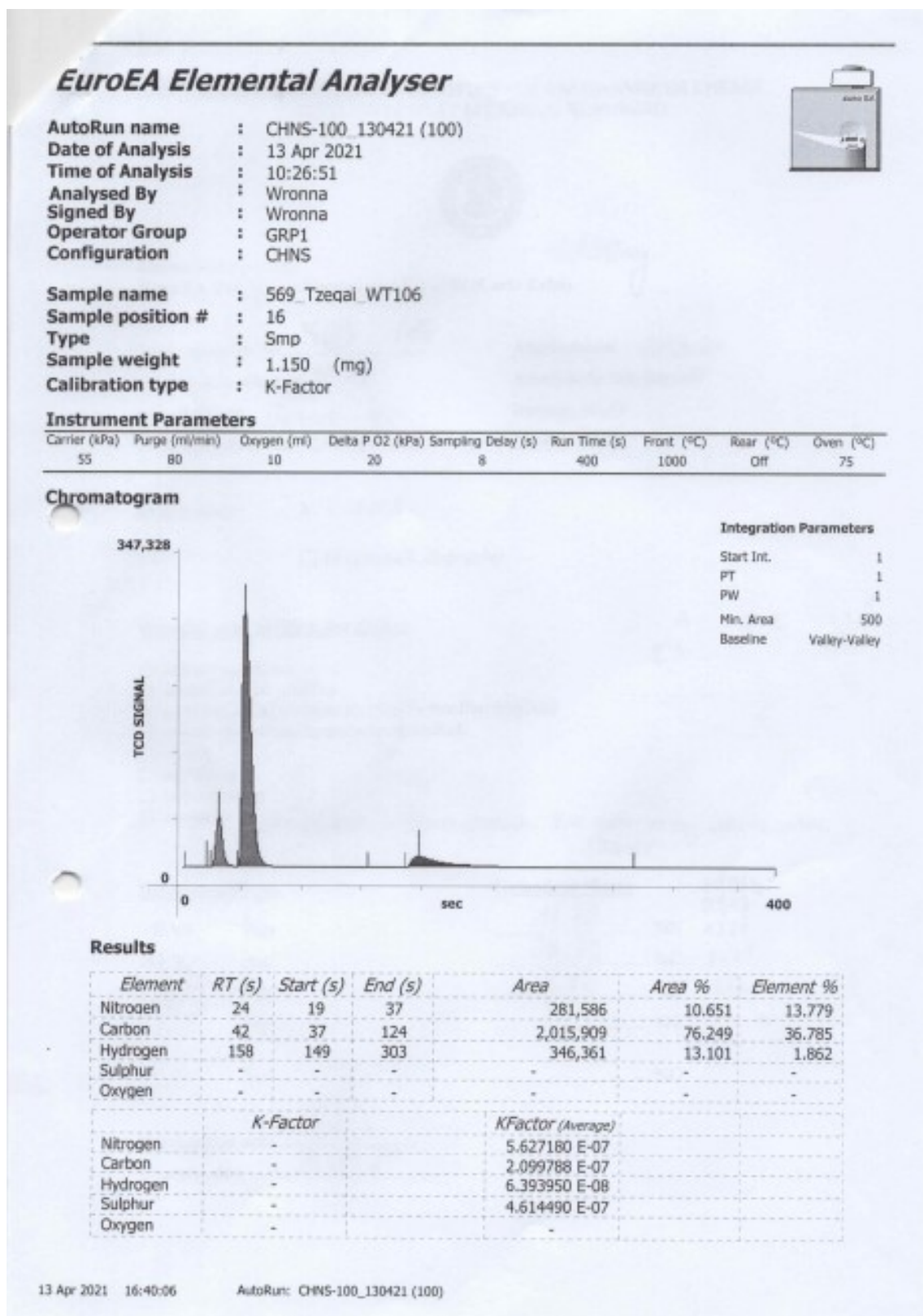


Figure S43. Elemental analysis of  $[\text{Mn}(\text{H}_2\text{bcpza})(\text{CO})_3]$  (**4**).

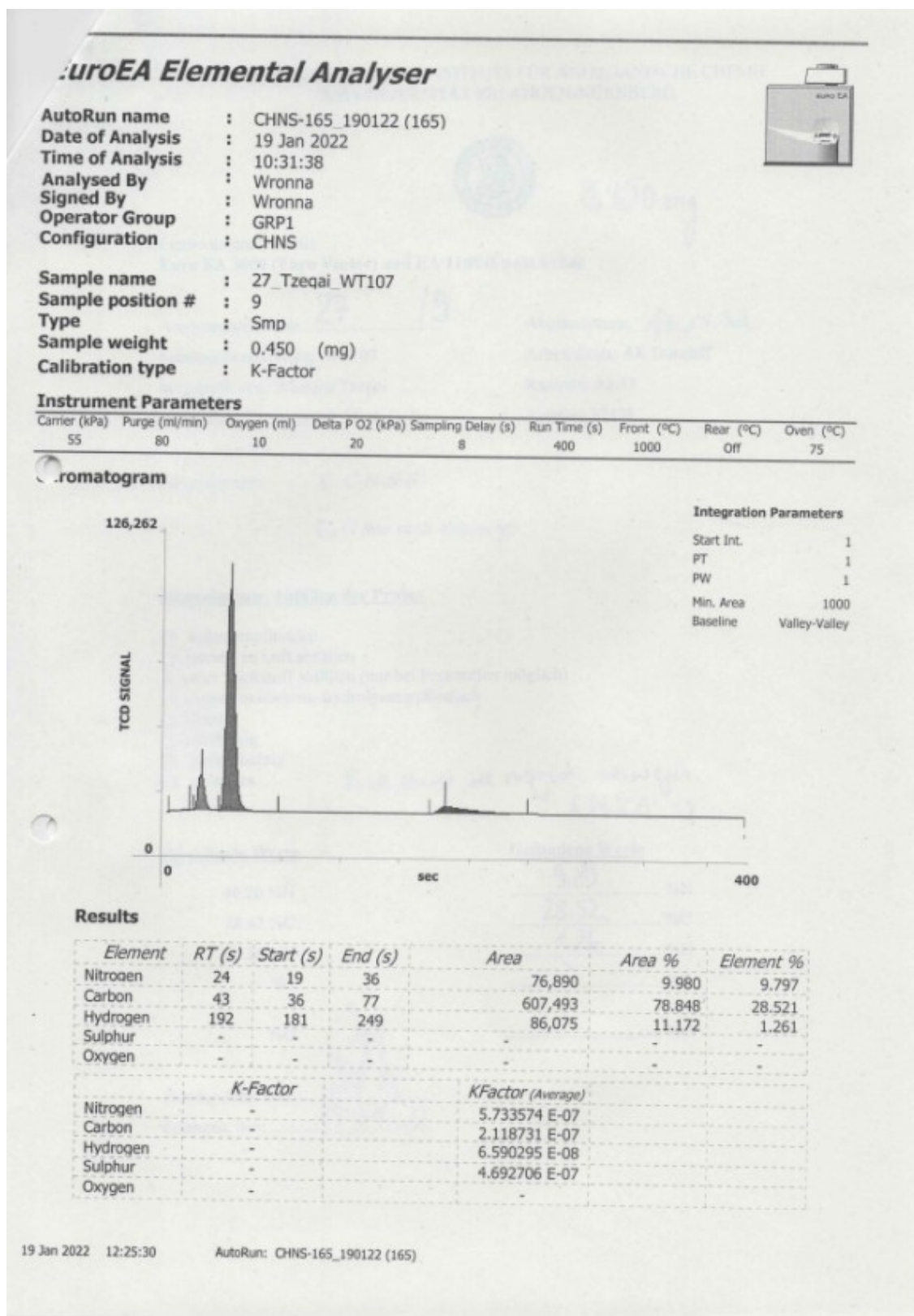


Figure S44. Elemental analysis of  $[\text{Re}(\text{H}_2\text{bcpza})(\text{CO})_3]$  (**5**).



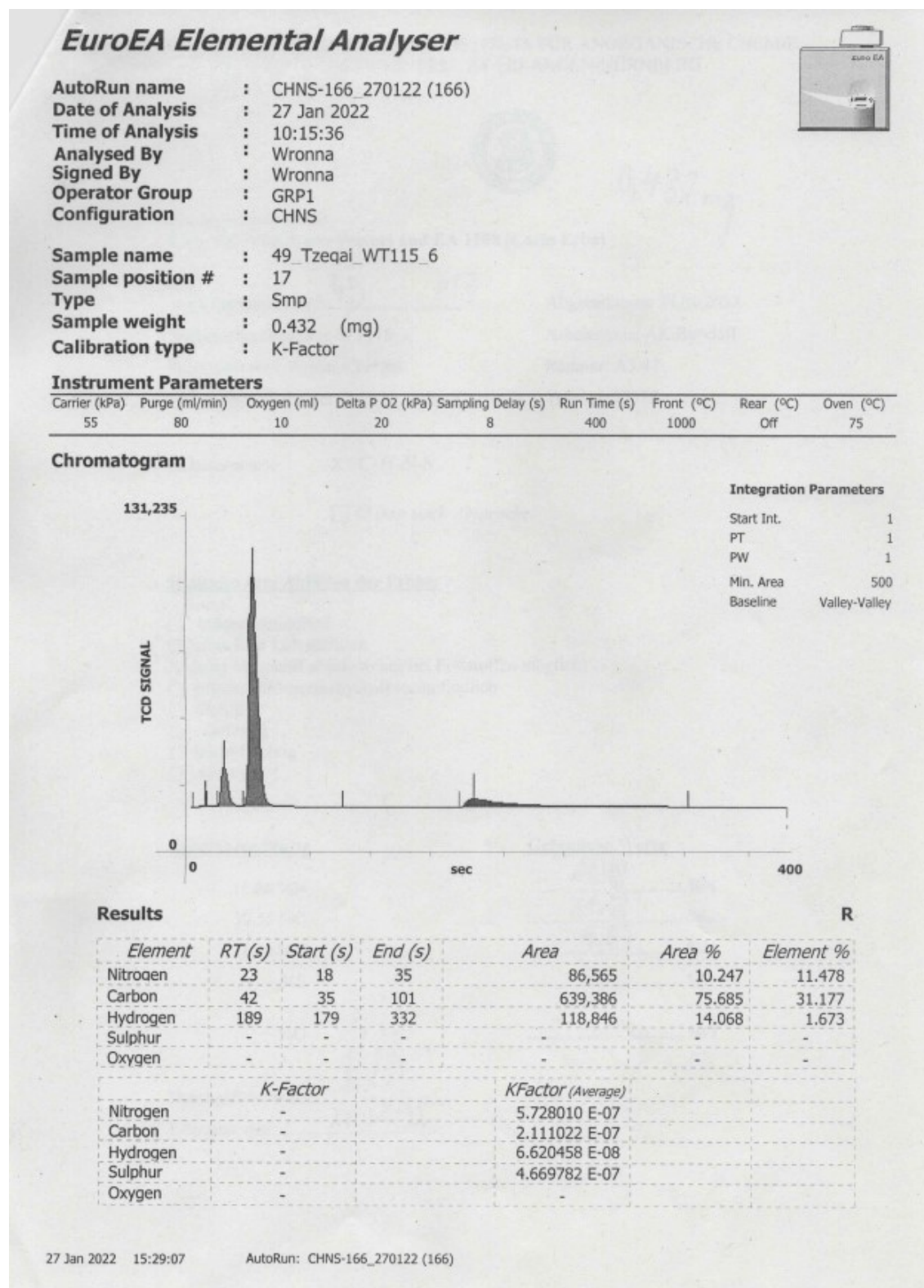


Figure S45. Elemental analysis of  $[\text{Ru}(\text{H}_2\text{bcpza})\text{Cl}(\text{CO})_2]$  (**6a**).

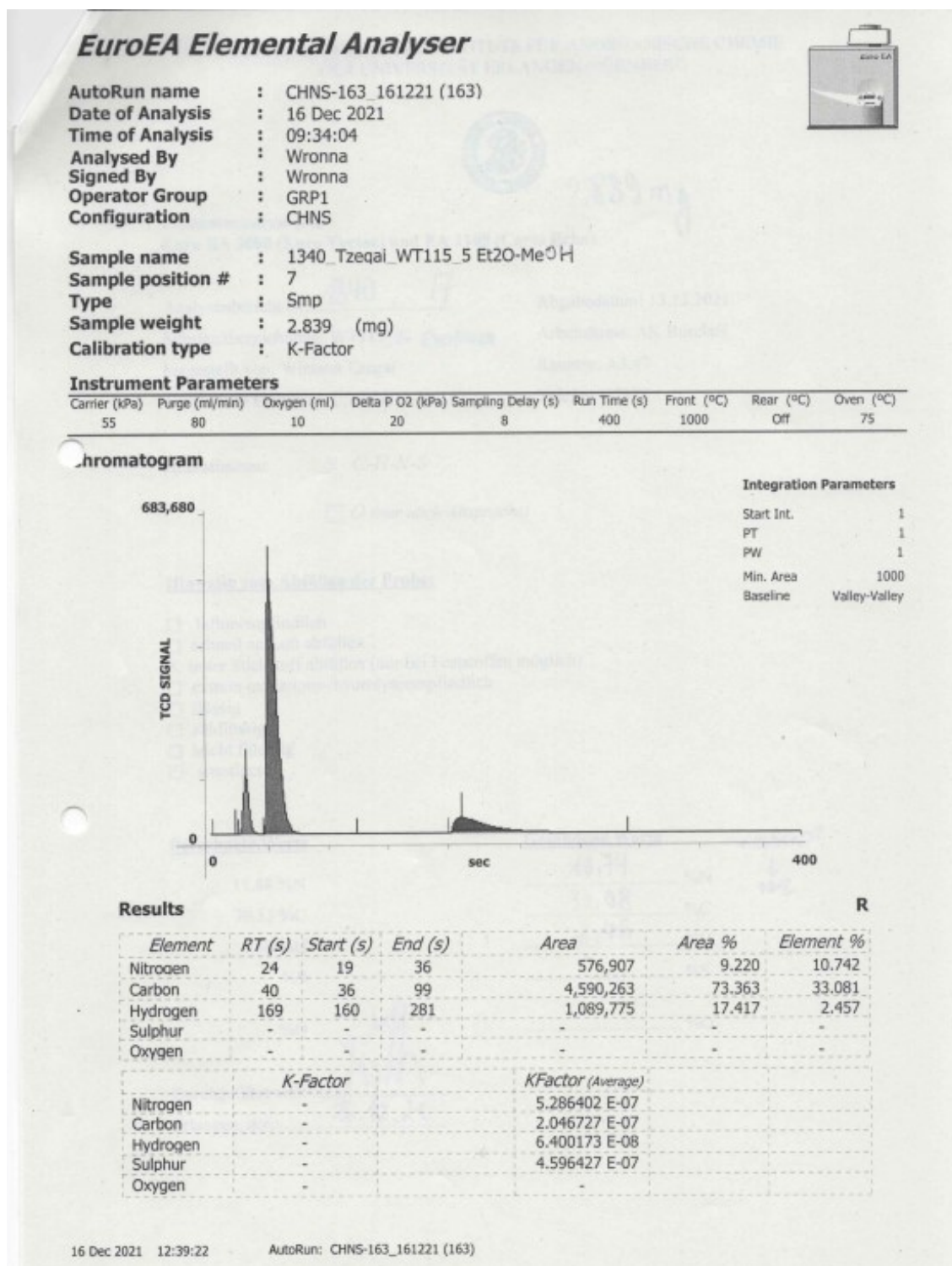


Figure S46. Elemental analysis of  $[\text{Ru}(\text{H}_2\text{bcpza})\text{Cl}(\text{CO})_2]$  (**6b**).